

RESEARCH

Open Access



# On the chaotic nature of the Rabinovich system through Caputo and Atangana–Baleanu–Caputo fractional derivatives

Chernet Tuge Deressa<sup>1\*</sup> 

\*Correspondence:

[chernet.deressa@ju.edu.et](mailto:chernet.deressa@ju.edu.et);  
[tugechernet@gmail.com](mailto:tugechernet@gmail.com)

<sup>1</sup> Department of Mathematics,  
College of Natural Sciences, Jimma  
University, Jimma, Ethiopia

## Abstract

The Rabinovich system can describe different physical interactions, including waves in plasmas, a convective fluid flow inside a rotating ellipsoid, and Kolmogorov's flow interactions. This study considers the Rabinovich system through Caputo and Atangana–Baleanu fractional derivatives to detect its chaotic nature. First, the existence and uniqueness of the solutions of the fractional-order systems are proved using the combination of the Picard–Lindelöf theorem and the Banach contraction principle. Then, a numerical approximation of the fractional systems is developed. The fractional Rabinovich system is found to exhibit a chaotic behavior verified via Lyapunov exponents. However, the fractional-order models do not enter into chaotic behavior at the same fractional-derivative order. Bifurcation diagrams referring to variation of the fractional-order derivatives are provided. Chaotic attractors for both cases of the fractional-derivative representation of the system are depicted. The two fractional-order models of the system show sensitivity to initial conditions. A master–response synchronization was developed in the context of the Atangana–Baleanu fractional derivative. The master and the response systems showed a strong correlation, proving the system's applicability in solving real problems, including secure communications.

**Keywords:** Rabinovich system; Atangana–Baleanu fractional derivative; Caputo fractional derivative; Chaos; Lyapunov exponents; Kaplan–Yorke dimension; Bifurcation diagram; Synchronization

## 1 Introduction

Fractional calculus was introduced as a branch of mathematical analysis in 1965, about the same time as the introduction of integral calculus. However, fractional calculus has started to gain much attention among researchers relatively recently in the last few decades. Since then, fractional calculus has been applied in different areas, including mathematical epidemiology [1], chaotic and hyperchaotic systems [2, 3], diffusion models, circuits [4], and so on.

© The Author(s) 2022. **Open Access** This article is licensed under a Creative Commons Attribution 4.0 International License, which permits use, sharing, adaptation, distribution and reproduction in any medium or format, as long as you give appropriate credit to the original author(s) and the source, provide a link to the Creative Commons licence, and indicate if changes were made. The images or other third party material in this article are included in the article's Creative Commons licence, unless indicated otherwise in a credit line to the material. If material is not included in the article's Creative Commons licence and your intended use is not permitted by statutory regulation or exceeds the permitted use, you will need to obtain permission directly from the copyright holder. To view a copy of this licence, visit <http://creativecommons.org/licenses/by/4.0/>.

There are several concepts of fractional derivatives in the literature, including Caputo fractional derivatives, Reimann–Liouville fractional derivatives, Caputo–Fabrizio fractional derivatives, and Atangana–Baleanu fractional derivatives, and so on.

Fractional derivatives can be grouped as singular kernels fractional derivatives, including Caputo fractional derivatives and Reimann–Liouville fractional derivatives, and non-singular kernels fractional derivatives, including Atangana–Baleanu–Caputo (ABC) and Caputo–Fabrizio fractional derivatives. Moreover, some of the fractional derivatives allow the inclusion of classical initial conditions (Caputo and ABC fractional derivatives), but Caputo–Fabrizio does not allow the inclusion of initial conditions in the usual sense [2, 3]. There are several advantages of using fractional derivatives compared to integer derivatives to analyze different dynamical systems; see [2, 3] and the references therein.

Chaos is a dynamic property that can be exhibited by nonlinear dynamic system characterized by sensitivity to initial conditions and parameter changes, bifurcation and period doubling, fraction Kaplan–Yorke dimension, dense orbits and transitivity, and expansivity [5, 6]. Many researchers are attracted to chaos theory and its applications in different areas, including secure communications [7], synchronization [8], image encryption [9], psychology [10], modeling financial and circuit systems [2], and so on. As a result, several research studies have been conducted on analyzing chaotic systems using different concepts of fractional derivatives: A Lorenz-like chaotic system is developed and analyzed via the Caputo fractional-derivative concept by Alam et al. [11]. The Caputo fractional-derivative concept is applied to study a chaotic nature and bifurcation of a simplified Lorenz system in [12]. Kumar et al. [13] used a bifurcation diagram and Lyapunov exponents to justify the chaotic nature of the 3D Rabinovich–Fabrikant system and a sliding mode control strategy to establish synchronization between two identical copies of the system. Hidden attractors and finite-time Lyapunov dimensions of the Rabinovich system are considered using integer derivatives [14]. The ABC and Caputo fractional derivatives are used to analyze different dynamic systems including systems of partial differential equations in [15–17].

To the best of the author’s knowledge, the Rabinovich system is not investigated via ABC and Caputo fractional-derivative concepts. Motivated by this and the potential of fractional derivatives in revealing hidden properties of a dynamic system, this study focuses on the qualitative analysis of the Rabinovich system through the Caputo and ABC fractional-derivative concepts.

The fractional Rabinovich system is considered to detect its chaotic nature via the memory-effect properties of the system. The memory effect of the system can be accounted for by applying different concepts of the fractional derivatives mentioned above. Accordingly, the integer-order Rabinovich system is represented by the ABC and Caputo fractional derivatives. The choice of these two fractional-derivative concepts is attributed to the possibility of including initial conditions in the system dynamics. Moreover, in the case of the Caputo fractional derivative, there is a Matlab code for generating bifurcation diagrams, Lyapunov exponents, and phase-portrait plots.

The existence and uniqueness of the solution of the fractional-order Rabinovich system are addressed using the concept of the Banach contraction principle. The predictor–corrector and Toufik–Atangana numerical approximations for the Rabinovich system’s Caputo and ABC fractional representations are used. The Matignon criterion for local stability analysis of systems of fractional derivatives is used [18].

The Lyapunov exponents, bifurcation diagrams, and different phase portraits of the Rabinovich system through Caputo and ABC fractional-derivative representations are obtained to confirm the impact of variation of the derivative orders and different parameter values. The sensitivity to initial conditions is also examined for Caputo and ABC representations of the Rabinovich system. A computer software Matlab 2018a is used for all the simulation results obtained in this study. Finally, a master–response synchronization through ABC representation of the Rabinovich system is established.

This report is organized as follows: The second section recaps the study's basic definitions and fractional-derivative concepts. Then, the Caputo fractional-derivative and the ABC fractional-derivative representation of the Rabinovich system is accomplished in the paper's third section. The fourth section details the existence and uniqueness of the fractional-derivative model of the system. Numerical approximation of the fractional-order systems is performed in the paper's fifth section. In the sixth section, the dynamic analysis of the fractional-derivative representations of the Rabinovich system is completed. Moreover, the local stability analysis, Lyapunov exponents, Kaplan–Yorke dimension, bifurcation diagrams, time-series solutions, attractors, and sensitivity to initial conditions are well thought out. The seventh section of the report is devoted to establishing a master–response synchronization process of the ABC fractional-order representation of the Rabinovich system. Finally, the conclusion is given, followed by a list of references.

## 2 Basic definitions and theorems

This section summarizes the definitions of fractional-derivative operators used in the study: The Atangana–Baleanu–Caputo (ABC), the Caputo fractional derivatives (C), and the Riemann–Liouville fractional derivative.

**Definition 1** ([1, 19]) For a fractional-derivative order  $\mu \in (0, 1]$ , and a function,  $g \in C^1(0, T)$ ,  $0 < T$ , the Atangana–Baleanu fractional derivative in the sense of the Caputo (ABC) fractional derivative is defined as:

$${}_0^{ABC}D_t^\mu g(t) = \frac{F(\mu)}{1-\mu} \int_0^t E_\mu \left[ -\frac{\mu}{1-\mu} (t-\tau)^\mu \right] \frac{dg}{d\tau}(\tau) d\tau, \quad (1)$$

where  $F(\mu) = 1 - \mu + \eta/\Gamma(\mu)$  is the normal operator,  $E_\mu(\cdot)$  represents the Mittag–Leffler function, and  $\Gamma(\cdot)$  denotes the Euler Gamma function.

**Theorem 1** ([1, 19]) *The time-fractional ordinary differential equation:*

$${}_0^{ABC}D_t^\mu g(t) = x(t), \quad (2)$$

*has a unique solution given by*

$$g(t) = \frac{1-\mu}{F(\mu)} x(t) + \frac{\mu}{F(\mu)\Gamma(\mu)} \int_0^t x(\rho)(t-\rho)^{\mu-1} d\rho.$$

**Definition 2** ([1, 19]) The ABC fractional-integral associate of the ABC fractional derivative is given by:

$${}_0^{ABC}I_t^\mu \{g(t)\} = \frac{1-\mu}{F(\mu)} g(t) + \frac{\mu}{F(\mu)\Gamma(\mu)} \int_0^t g(\rho)(t-\rho)^{\mu-1} d\rho. \quad (3)$$

**Definition 3** ([20, 21]) For a fractional-derivative order  $\mu \in (0, 1]$ , and a function  $g \in C^1(0, T)$ ,  $0 < T$ , the Caputo fractional derivative is defined as:

$${}^C D_t^\eta g(t) = \frac{1}{\Gamma(1-\eta)} \int_0^t (t-\tau)^{-\eta} \frac{d}{d\tau} g(\tau) d\tau, \quad \eta \in (0, 1), t > 0. \quad (4)$$

**Definition 4** ([1, 19]) For a fractional-derivative order  $\mu \in (0, 1]$ , and a function  $g \in C^1(0, T)$ ,  $0 < T$ , the Riemann–Liouville fractional-integral operator is defined as

$${}^{RL} I_t^\mu f(t) = \frac{1}{\Gamma(\mu)} \int_0^t (t-\tau)^{\mu-1} g(\tau) d\tau. \quad (5)$$

**Definition 5** ([1, 19]) For a fractional-derivative order  $\mu \in (0, 1]$ , and a function  $g \in C^1(0, T)$ ,  $0 < T$ , the Riemann–Liouville fractional derivative is defined as

$${}^{RL} D_t^\mu g(t) = \frac{1}{\Gamma(1-\mu)} \frac{d}{dt} \int_0^t (t-\tau)^{-\mu} g(\tau) d\tau. \quad (6)$$

### 3 ABC and Caputo fractional-derivative representations of the Rabinovich system

In 1978 Rabinovich studied a system named after him that is given in Eq. (7), [14]

$$\begin{cases} \dot{x} = ay - bx - yz, \\ \dot{y} = ax - cy + xz, \\ \dot{z} = -z + xy, \end{cases} \quad (7)$$

where  $a, b$ , and  $c$  are positive parameters. The application of the Rabinovich system and the physical meaning of the parameters are described in [14]. More importantly, it can be used to describe several physical interactions, including waves in plasma interactions, the interaction of a convective fluid flow inside a rotating ellipsoid, and Kolmogorov's flow, to list just a few. A linear transformation and time scaling of (7) using  $x \rightarrow bcy/a, y \rightarrow bx, z \rightarrow bcz/a, t \rightarrow t/a$ , leads to the system shown in (8)

$$\begin{cases} \dot{x} = \beta(y - x) - \delta yz, \\ \dot{y} = \alpha x - y - xz, \\ \dot{z} = -\gamma z + xy, \end{cases} \quad (8)$$

where  $\beta = c/b, \gamma = 1/b, \delta = -c^2/a^2, \alpha = a^2/bc$ , and  $\beta = -\delta\alpha$ .

It must be noted that three of the parameters in the system (8) are positive and  $\delta$  is negative. The 3D system in (8) for  $\delta = 0$  is the well-known Lorenz system.

In this study, the objective is to qualitatively analyze system (8) in the context of Caputo and ABC fractional derivatives. Accordingly, the ABC fractional-derivative representation and the Caputo fractional-derivative representation of the Rabinovich system (8) are, respectively, given in Eqs. (9) and (10).

Let

$$H_1(x, y, z, t) = \beta(y - x) - \delta yz,$$

$$H_2(x, y, z, t) = \alpha x - y - xz,$$

$$H_3(x, y, z, t) = -\gamma z + xy,$$

$$\begin{cases} {}_0^{ABC}D_t^\mu x(t) = H_1(x, y, z, t), \\ {}_0^{ABC}D_t^\mu y(t) = H_2(x, y, z, t), \\ {}_0^{ABC}D_t^\mu z(t) = H_3(x, y, z, t), \end{cases} \quad (9)$$

$$\begin{cases} {}_0^CD_t^\mu x(t) = H_1(x, y, z, t), \\ {}_0^CD_t^\mu y(t) = H_2(x, y, z, t), \\ {}_0^CD_t^\mu z(t) = H_3(x, y, z, t), \end{cases} \quad (10)$$

with initial conditions  $X(0) = (x(0), y(0), z(0))$ .

#### 4 Existence and uniqueness of solutions of the fractional-derivative order Rabinovich system

This section proves the existence and uniqueness of a solution of the system (9) via the Banach fixed-point theorem and the Banach contraction principle [2, 3, 22].

Note that since  $H_1$ ,  $H_2$ , and  $H_3$  defined in (9) are all continuous everywhere in  $\mathbb{R}^3$ , the existence of at least one solution for system (9) is guaranteed. We now show the uniqueness of the solution for the given initial condition shown in (9) by defining Picard's operator and the principle of contraction mapping. Since, Lipschitz continuity is the main condition for Picard–Lindelöf's theorem that guarantees the existence and uniqueness of system of differential equations such as (9), we show whether each of the equations in (9) satisfies Lipschitz continuity followed by defining Picard's operator.

First, it is shown that the first equation of (9) satisfies the condition of Lipschitz continuity; demonstrated in the following procedure:

$$\begin{aligned} \|H_1(x_1, y, z, t) - H_1(x_2, y, z, t)\| &= \|\beta(y - x_1) - \delta yz - \beta(y - x_2) + \delta yz\| \\ &\leq \beta\|x_2 - x_1\|. \end{aligned} \quad (11)$$

Hence, the Lipschitz continuity is satisfied with the Lipschitz constant  $\beta$ . This result assures that the first equation of (9) has at least one solution.

Secondly, Picard's operator is set up as follows: Applying the fundamental theorem of calculus to the first equation of (9),  ${}_0^{ABC}D_t^\mu x(t) = H_1(x, y, z, t)$ , we obtain

$$x(t) - x(0) = {}_0^{ABC}I_t^\mu \{H_1(x, y, z, t)\}.$$

Assuming that  $P$  is Picard's operator, we have

$$Px(t) - x(0) = {}_0^{ABC}I_t^\mu \{H_1(x, y, z, t)\}.$$

The boundedness of Picard's operator  $P$ , is shown as follows:

$$\|Px(t) - x(0)\| = \|{}_0^{ABC}I_t^\mu \{H_1(x, y, z, t)\}\| \leq {}_0^{ABC}I_t^\mu \|H_1(x, y, z, t)\|. \quad (12)$$

Since it is proved that  $H_1(x, y, z, t)$  is Lipschitz continuous, we have  $H_1(x, y, z, t)$  is bounded, and thus there is a constant  $k_1$  such that  $\|H_1(x, y, z, t)\| \leq k_1$ . Consequently, Eq. (12) becomes

$$\begin{aligned}\|Px(t) - x(0)\| &= \|{}_0^{ABC}I_t^\mu \{H_1(x, y, z, t)\}\| \leq {}_0^{ABC}I_t^\mu \|H_1(x, y, z, t)\| \\ &\leq k_1 ({}_0^{ABC}I_t^\mu (1)) \\ &\leq k_1 \left( \frac{1-\mu}{F(\mu)} + \frac{T^\mu}{F(\mu)\Gamma(\mu)} \right), \quad \exists T, t \leq T.\end{aligned}$$

The boundedness of the operator  $P$  is thus proved.

Thirdly, a condition for the operator  $P$  to be a contraction mapping is developed as follows:

$$\begin{aligned}\|Px_1(t) - Px_2(t)\| &= \|{}_0^{ABC}I_t^\mu \{H_1(x_1, y, z, t) - H_1(x_2, y, z, t)\}\| \\ &\leq \|H_1(x_1, y, z, t) - H_1(x_2, y, z, t)\| {}_0^{ABC}I_t^\mu (1) \\ &\leq \beta \|x_1(t) - x_2(t)\| ({}_0^{ABC}I_t^\mu (1)) \\ &\leq \beta \left( \frac{1-\mu}{F(\mu)} + \frac{T^\mu}{F(\mu)\Gamma(\mu)} \right) \|x_1(t) - x_2(t)\|, \quad \exists T, t \leq T.\end{aligned}$$

Thus, the operator  $P$  is a contraction mapping if the following condition is satisfied:

$$\left( \frac{1-\mu}{F(\mu)} + \frac{T^\mu}{F(\mu)\Gamma(\mu)} \right) \leq \frac{1}{\beta}. \quad (13)$$

The uniqueness of the solution is proved as follows:

Let us assume that  $x_1(t)$  and  $x_2(t)$  are two solutions to the first equation in (9). Then, we have

$$\begin{aligned}x_1(t) - x_1(0) &= {}_0^{ABC}I_t^\mu \{H_1(x_1, y, z, t)\}, \\ x_2(t) - x_2(0) &= {}_0^{ABC}I_t^\mu \{H_1(x_2, y, z, t)\}.\end{aligned} \quad (14)$$

Considering the difference between the two solutions, assuming the two solutions have the same initial point, and taking the Euclidian norm, we obtain

$$\begin{aligned}\|x_1(t) - x_2(t)\| &= \|{}_0^{ABC}I_t^\mu \{H_1(x_1, y, z, t) - H_1(x_2, y, z, t)\}\| \\ &\leq {}_0^{ABC}I_t^\mu \|H_1(x_1, y, z, t) - H_1(x_2, y, z, t)\| \\ &\leq \beta \left( \frac{1-\mu}{F(\mu)} + \frac{T^\mu}{F(\mu)\Gamma(\mu)} \right) \|x_1(t) - x_2(t)\|.\end{aligned}$$

Thus, we have the following relation:

$$\|x_1(t) - x_2(t)\| \left[ 1 - \beta \left( \frac{1-\mu}{F(\mu)} + \frac{T^\mu}{F(\mu)\Gamma(\mu)} \right) \right] \leq 0. \quad (15)$$

It then follows that  $\|x_1(t) - x_2(t)\| \leq 0$  and hence that  $x_1(t) = x_2(t)$ .

We continue the process of demonstrating the existence and uniqueness of the solution of (9) with the second equation.

Secondly, it is shown that the second equation of (9) satisfies the condition of Lipschitz continuity; demonstrated in the following procedure:

$$\|H_2(x, y_1, z, t) - H_2(x, y_2, z, t)\| = \|\alpha x - y_1 - xz - \alpha x + y_2 + xz\| \leq \|y_2 - y_1\|.$$

Hence, the Lipschitz continuity is satisfied with the Lipschitz constant of 1 and Picard's operator is set up as follows: From the second equation of (9) we have

$$y(t) - y(0) = {}_0^{ABC}I_t^\mu \{H_2(x, y, z, t)\}.$$

Assuming that  $Q$  is Picard's operator, we obtain

$$Qy(t) - y(0) = {}_0^{ABC}I_t^\mu \{H_2(x, y, z, t)\}.$$

The boundedness of Picard's operator  $Q$ , is shown as follows:

$$\|Qy(t) - y(0)\| = \|{}_0^{ABC}I_t^\mu \{H_2(x, y, z, t)\}\| \leq {}_0^{ABC}I_t^\mu \|H_2(x, y, z, t)\|. \quad (16)$$

Since it is proved that  $H_2(x, y, z, t)$  is Lipschitz continuous, we have  $H_2(x, y, z, t)$  is bounded, and thus there is a constant  $k$  such that  $\|H_2(x, y, z, t)\| \leq k$ . Consequently, Eq. (16) becomes

$$\begin{aligned} \|Qx(t) - x(0)\| &= \|{}_0^{ABC}I_t^\mu \{H_2(x, y, z, t)\}\| \leq {}_0^{ABC}I_t^\mu \|H_2(x, y, z, t)\| \\ &\leq k({}_0^{ABC}I_t^\mu(1)) \\ &\leq k\left(\frac{1-\mu}{F(\mu)} + \frac{T^\mu}{F(\mu)\Gamma(\mu)}\right), \quad \exists T \in \mathbb{R}, t \leq T. \end{aligned}$$

Thus, the boundedness of the operator  $Q$  is proved.

We developed a condition for the operator  $Q$  to be a contraction mapping as follows:

$$\begin{aligned} \|Qy_1(t) - Qy_2(t)\| &= \|{}_0^{ABC}I_t^\mu \{H_2(x, y_1, z, t) - H_2(x, y_2, z, t)\}\| \\ &\leq \|H_2(x, y_1, z, t) - H_2(x, y_2, z, t)\| {}_0^{ABC}I_t^\mu(1) \\ &\leq \|y_1(t) - y_2(t)\| ({}_0^{ABC}I_t^\mu(1)) \\ &\leq \left(\frac{1-\mu}{F(\mu)} + \frac{h^\mu}{F(\mu)\Gamma(\mu)}\right) \|y_1(t) - y_2(t)\|, \quad \exists h \in \mathbb{R} \text{ and } t \leq h. \end{aligned}$$

Thus, Picard's operator  $Q$  is a contraction mapping if the following condition is satisfied:

$$\frac{1-\mu}{F(\mu)} + \frac{h^\mu}{F(\mu)\Gamma(\mu)} \leq 1. \quad (17)$$

Lastly, the uniqueness of the solution is proved as follows:

Let us assume that  $y_1(t)$  and  $y_2(t)$  are two solutions to the first equation in (9). Then, we have

$$\begin{aligned} y_1(t) - y_1(0) &= {}_0^{ABC}I_t^\mu \{H_2(x, y_1, z, t)\}, \\ y_2(t) - y_2(0) &= {}_0^{ABC}I_t^\mu \{H_2(x, y_2, z, t)\}. \end{aligned} \quad (18)$$

Considering the difference between the two solutions, assuming the two solutions have the same initial point, and taking the Euclidian norm, we obtain

$$\begin{aligned} \|y_1(t) - y_2(t)\| &= \|{}_0^{ABC}I_t^\mu \{H_2(x, y_1, z, t) - H_2(x, y_2, z, t)\}\| \\ &\leq {}_0^{ABC}I_t^\mu \|\{H_2(x, y_1, z, t) - H_2(x, y_2, z, t)\}\| \\ &\leq \left( \frac{1-\mu}{F(\mu)} + \frac{h^\mu}{F(\mu)\Gamma(\mu)} \right) \|y_1(t) - y_2(t)\|. \end{aligned}$$

Thus, we have the following relation:

$$\|y_1(t) - y_2(t)\| \left[ 1 - \left( \frac{1-\mu}{F(\mu)} + \frac{h^\mu}{F(\mu)\Gamma(\mu)} \right) \right] \leq 0.$$

It then follows that  $\|y_1(t) - y_2(t)\| \leq 0$  and  $y_1(t) = y_2(t)$ .

Thirdly, it is shown that the third equation of (9) satisfies the condition of Lipschitz continuity demonstrated in the following procedure:

$$\|H_3(x, y, z_1, t) - H_3(x, y, z_2, t)\| = \|- \gamma z_1 + xy + \gamma z_2 - xy\| \leq \gamma \|z_2 - z_1\|.$$

Hence, the Lipschitz continuity is satisfied with the Lipschitz constant of  $\gamma$ . We set up Picard's operator as follows: From the third equation we have

$$z(t) - z(0) = {}_0^{ABC}I_t^\mu \{H_3(x, y, z, t)\}.$$

Assuming that  $R$  is a Picard's operator, we obtain

$$Ry(t) - y(0) = {}_0^{ABC}I_t^\mu \{H_3(x, y, z, t)\}.$$

The boundedness of Picard's operator  $R$  is shown as follows:

$$\|Rz(t) - z(0)\| = \|{}_0^{ABC}I_t^\mu \{H_3(x, y, z, t)\}\| \leq {}_0^{ABC}I_t^\mu \|\{H_3(x, y, z, t)\}\|. \quad (19)$$

Since it is proved that  $H_3(x, y, z, t)$  is Lipschitz continuous, we have  $H_3(x, y, z, t)$  bounded, and thus there is a constant  $r$  such that  $\|\{H_3(x, y, z, t)\}\| \leq r$ . Consequently, Eq. (19) becomes

$$\begin{aligned} \|Rx(t) - x(0)\| &= \|{}_0^{ABC}I_t^\mu \{H_3(x, y, z, t)\}\| \leq {}_0^{ABC}I_t^\mu \|\{H_3(x, y, z, t)\}\| \\ &\leq r({}_0^{ABC}I_t^\mu(1)) \\ &\leq r\left(\frac{1-\mu}{F(\mu)} + \frac{p^\mu}{F(\mu)\Gamma(\mu)}\right), \quad \exists p \in \mathbb{R}, t \leq p. \end{aligned}$$



The boundedness of the operator  $R$  is then proved.

Next, a condition for the operator  $R$  to be a contraction mapping is developed as follows:

$$\begin{aligned}\|Rz_1(t) - Rz_2(t)\| &= \|{}_0^{ABC}I_t^\mu \{H_3(x, y, z_1, t) - H_3(x, y, z_2, t)\}\| \\ &\leq \| \{H_3(x, y, z_1, t)\} - \{H_3(x, y, z_2, t)\} \| {}_0^{ABC}I_t^\mu(1) \\ &\leq \|z_1(t) - z_2(t)\| ({}_0^{ABC}I_t^\mu(1)) \\ &\leq r \left( \frac{1-\mu}{F(\mu)} + \frac{p^\mu}{F(\mu)\Gamma(\mu)} \right) \|z_1(t) - z_2(t)\|, \quad \exists p \in \mathbb{R} \text{ and } t \leq p.\end{aligned}$$

Thus, Picard's operator  $R$  is a contraction mapping if the following condition is satisfied:

$$\left( \frac{1-\mu}{F(\mu)} + \frac{p^\mu}{F(\mu)\Gamma(\mu)} \right) \leq \frac{1}{r}. \quad (20)$$

Lastly, the uniqueness of the solution is proved as follows:

Let us assume that  $z_1(t)$  and  $z_2(t)$  are two solutions to the first equation in (9). Then, we have

$$\begin{aligned}z_1(t) - z_1(0) &= {}_0^{ABC}I_t^\mu \{H_3(x, y, z_1, t)\}, \\ z_2(t) - z_2(0) &= {}_0^{ABC}I_t^\mu \{H_3(x, y, z_2, t)\}.\end{aligned} \quad (21)$$

Considering the difference between the two solutions, assuming the two solutions have the same initial point, and taking the Euclidian norm, we obtain

$$\begin{aligned}\|z_1(t) - z_2(t)\| &= \|{}_0^{ABC}I_t^\mu \{H_3(x, y, z_1, t) - H_3(x, y, z_2, t)\}\| \\ &\leq {}_0^{ABC}I_t^\mu \| \{H_3(x, y, z_1, t) - H_3(x, y, z_2, t)\} \| \\ &\leq r \left( \frac{1-\mu}{F(\mu)} + \frac{p^\mu}{F(\mu)\Gamma(\mu)} \right) \|z_1(t) - z_2(t)\|.\end{aligned}$$

Thus, we have the following relation:

$$\|z_1(t) - z_2(t)\| \left[ 1 - r \left( \frac{1-\mu}{F(\mu)} + \frac{p^\mu}{F(\mu)\Gamma(\mu)} \right) \right] \leq 0.$$

It then follows that  $\|z_1(t) - z_2(t)\| \leq 0$  and  $z_1(t) = z_2(t)$ .

We proved that all the operators  $P$ ,  $Q$ , and  $R$  are well defined and contraction mappings. Thus, the system (9) in the context of the Atangana–Baleanu fractional derivative has a unique solution for a given initial condition. The case of the system (10) in the context of the Caputo fractional derivative can be proved similarly.

## 5 Numerical approximation of the fractional-order Rabinovich system

### 5.1 Numerical approximation of the ABC fractional-derivative representation of the Rabinovich system

The Toufik–Atangana numerical scheme [23] is applied to the ABC representation of the Rabinovich system as follows:

Referring to Theorem 1 and the first equation of (9), we have the solution of (22) given in (23)

$${}_0^{ABC}D_t^\alpha x(t) = H_1(x(t), y(t), z(t), t), \quad x_0 = x(0), \quad (22)$$

$$\begin{aligned} x(t) = & x(0) + \frac{1-\mu}{F(\mu)} H_1(x(t), y(t), z(t), t) \\ & + \frac{\mu}{F(\mu)\Gamma(\mu)} \int_0^t H_1(\rho, x(\rho), y(\rho), z(\rho))(t-\rho)^{\mu-1} d\rho. \end{aligned} \quad (23)$$

The integral part in (23) is approximated by Lagrange's interpolation polynomial in  $[t_k, t_{k+1}]$  to

$$H_1(x, y, z, t) = \beta(y - x) - \delta yz,$$

which leads to

$$x_k \approx \frac{1}{h} \left[ (s - t_{k-1}) H_1(x(t_k), y(t_k), z(t_k)) - (s - t_k) H_1(x(t_{k-1}), y(t_{k-1}), z(t_{k-1})) \right], \quad (24)$$

where  $h = t_k - t_{k-1}$ .

After substituting (24) into (23), we obtain the expression in (25)

$$\begin{aligned} x(t_{n+1}) &= x(0) + \frac{1-\mu}{F(\mu)} H_1(x(t_k), y(t_k), z(t_k)) \\ &+ \frac{\mu}{F(\mu)\Gamma(\mu)} \sum_{j=1}^n \left( \frac{H_1(x(t_j), y(t_j), z(t_j))}{h} \Omega_{j-1} - \frac{H_1(x(t_{j-1}), y(t_{j-1}), z(t_{j-1}))}{h} \Omega_j \right), \end{aligned} \quad (25)$$

where

$$\begin{aligned} \Omega_{j-1} &= \int_{t_j}^{t_{j+1}} (s - t_{j-1})(t_{n+1} - s)^{\mu-1} ds \\ &= -\frac{1}{\mu} \left[ (t_{j+1} - t_{j-1})(t_{n+1} - t_{j+1})^\mu - (t_j - t_{j-1})(t_{n+1} - t_j)^\mu \right] \\ &\quad - \frac{1}{\mu(\mu+1)} \left[ (t_{n+1} - t_{j+1})^{\mu+1} (t_{n+1} - t_{j+1})^\mu - (t_{n+1} - t_j)^{\mu+1} \right], \end{aligned} \quad (26)$$

$$\begin{aligned} \Omega_j &= \int_{t_j}^{t_{j+1}} (y - t_{j-1})(t_{n+1} - s)^{\mu-1} ds \\ &= -\frac{1}{\mu} \left[ (t_{j+1} - t_{j-1})(t_{n+1} - t_{j+1})^\mu \right] \\ &\quad - \frac{1}{\mu(\mu+1)} \left[ (t_{n+1} - t_{j+1})^{\mu+1} - (t_{n+1} - t_j)^{\mu+1} \right]. \end{aligned} \quad (27)$$

If we substitute  $t_j = jh$  into (26) and (27), we obtain

$$\Omega_{j-1} = \frac{h^{\mu+1}}{\mu(\mu+1)} \left[ (n+1-j)^\mu (n-j+2+\mu) - (n-j)^\mu (n-j+2+2\mu) \right], \quad (28)$$

$$\Omega_j = \frac{h^{\mu+1}}{\mu(\mu+1)} [(n+1-j)^{\mu+1} - (n-j)^\mu (n-j+1+\mu)]. \quad (29)$$

Finally, Eq. (25) is expressed in terms of Eqs. (28) and (29) by Eq. (30):

$$\begin{aligned} x(t_{n+1}) &= x(0) + \frac{1-\mu}{F(\mu)} H_1(x(t_n), y(t_n), z(t_n)) \\ &\quad + \frac{\mu}{F(\mu)\Gamma(\mu)} \\ &\quad \times \sum_{j=1}^n \left( \begin{aligned} &\left( \frac{H_1(x(t_j), y(t_j), z(t_j))}{\Gamma(\mu+2)} \right) \\ &\times h^\mu [(n+1-j)^\mu (n-j+2+\mu) - (n-j)^\mu (n-j+2+2\mu)] \\ &- \left( \frac{H_1(x(t_{j-1}), y(t_{j-1}), z(t_{j-1}))}{\Gamma(\mu+2)} \right) \\ &\times h^\mu [(n+1-j)^{\mu+1} - (n-j)^\mu (n-j+1+\mu)] \end{aligned} \right). \end{aligned} \quad (30)$$

Similarly, we have the following numerical approximations for the remaining equations of (9):

$$\begin{aligned} y(t_{n+1}) &= y(0) + \frac{1-\mu}{F(\mu)} H_2(x(t_n), y(t_n), z(t_n)) \\ &\quad + \frac{\mu}{F(\mu)\Gamma(\mu)} \\ &\quad \times \sum_{j=1}^n \left( \begin{aligned} &\left( \frac{H_2(x(t_j), y(t_j), z(t_j))}{\Gamma(\mu+2)} \right) \\ &\times h^\mu [(n+1-j)^\mu (n-j+2+\mu) - (n-j)^\mu (n-j+2+2\mu)] \\ &- \left( \frac{H_2(x(t_{j-1}), y(t_{j-1}), z(t_{j-1}))}{\Gamma(\mu+2)} \right) \\ &\times h^\mu [(n+1-j)^{\mu+1} - (n-j)^\mu (n-j+1+\mu)] \end{aligned} \right), \end{aligned} \quad (31)$$

$$\begin{aligned} z(t_{n+1}) &= z(0) + \frac{1-\mu}{F(\mu)} H_3(x(t_n), y(t_n), z(t_n)) \\ &\quad + \frac{\mu}{F(\mu)\Gamma(\mu)} \\ &\quad \times \sum_{j=1}^n \left( \begin{aligned} &\left( \frac{H_3(x(t_j), y(t_j), z(t_j))}{\Gamma(\mu+2)} \right) \\ &\times h^\mu [(n+1-j)^\mu (n-j+2+\mu) - (n-j)^\mu (n-j+2+2\mu)] \\ &- \left( \frac{H_3(x(t_{j-1}), y(t_{j-1}), z(t_{j-1}))}{\Gamma(\mu+2)} \right) \\ &\times h^\mu [(n+1-j)^{\mu+1} - (n-j)^\mu (n-j+1+\mu)] \end{aligned} \right). \end{aligned} \quad (32)$$

The numerical approximation of the ABC representation of the Rabinovich system is given by Eqs. (30)–(32). Moreover, the stability and convergence of the formulation of the numerical approximation for ABC fractional derivatives are proved by Toufik and Atangana [23].

## 5.2 Predictor–corrector numerical approximation of the Caputo fractional-derivative representation of the Rabinovich system

This subsection explains the numerical approximation applied to the Caputo fractional-derivative representation of the Rabinovich system (10). The predictor-corrector method is used because it has a Matlab code to obtain phase portraits and time-series solutions.

Moreover, the method is proved stable and convergent and was first reported by Garrappa [24].

The numerical approximation by Garrappa [24] used the Reimann–Liouville fractional integral operator (5) for discretization. In the same manner, starting from the first equation of (10) and applying the Reimann–Liouville fractional integral operator for developing the approximation for model (10); as demonstrated as follows:

It is evident that the solutions of (10) are given by

$$\begin{cases} x(t) = x(0) + {}_0^{RL}I_t^\mu H_1(x, y, z, t), \\ y(t) = y(0) + {}_0^{RL}I_t^\mu H_2(x, y, z, t), \\ z(t) = z(0) + {}_0^{RL}I_t^\mu H_3(x, y, z, t). \end{cases} \quad (33)$$

The integral part of (33) is approximated by applying the predictor–corrector method that leads to

$$\begin{cases} x(t) = x(0) + h^\mu [\kappa_m^\mu H_1(0) + \sum_{j=1}^{m-1} \psi_{m-j}^\mu H_1(x_j, y_j, z_j, t_j) + \psi_0^\mu H_1(x_m^p, y_m^p, z_m^p, t_j)], \\ y(t) = y(0) + h^\mu [\kappa_m^\mu H_2(0) + \sum_{j=1}^{m-1} \psi_{m-j}^\mu H_2(x_j, y_j, z_j, t_j) + \psi_0^\mu H_2(x_m^p, y_m^p, z_m^p, t_j)], \\ z(t) = z(0) + h^\mu [\kappa_m^\mu H_3(0) + \sum_{j=1}^{m-1} \psi_{m-j}^\mu H_3(x_j, y_j, z_j, t_j) + \psi_0^\mu H_3(x_m^p, y_m^p, z_m^p, t_j)], \end{cases} \quad (34)$$

where,

$$\begin{aligned} \kappa_m^\mu &= \frac{(m-1)^\mu - m^\mu(m-\mu-1)}{\Gamma(2+\mu)}, \\ \psi_m^\mu &= \frac{(m-1)^{\mu+1} - 2m^{\mu+1} + m^\mu(m+1)}{\Gamma(2+\mu)}, \quad m = 1, 2, 3, \dots, \\ \psi_0^\mu &= \frac{1}{\Gamma(2+\mu)}. \end{aligned}$$

Moreover, the predictors are given as follows:

$$\begin{cases} x^p(t_m) = x(0) + h^\mu \sum_{j=1}^{m-1} \psi_{m-j-1}^\mu H_1(x_j, y_j, z_j, t_j), \\ y^p(t_m) = y(0) + h^\mu \sum_{j=1}^{m-1} \psi_{m-j-1}^\mu H_2(x_j, y_j, z_j, t_j), \\ z^p(t_m) = z(0) + h^\mu \sum_{j=1}^{m-1} \psi_{m-j-1}^\mu H_3(x_j, y_j, z_j, t_j). \end{cases} \quad (35)$$

The predictor–corrector method is applied to obtain the attractor and time-series solutions of (10). In addition, the Danca algorithm [25] is used to obtain the Lyapunov exponents of (10). ‘The code is developed to determine all Lyapunov exponents of a class fractional-order system modeled by the Caputo fractional derivative. The predictor–corrector Adams–Bashforth–Moulton numerical method is the underlying numerical method used in the code.’

## 6 Dynamic analysis of the fractional-order Rabinovich system

### 6.1 Local stability analysis of the fractional Rabinovich system

This section is devoted to the local stability analysis of the Rabinovich model in the context of fractional derivatives (9) and (10). The Matignon criterion is used for the local stability analysis of the system. According to the criterion, a fractional-order system is said to

be locally asymptotically stable if all the eigenvalues of the Jacobian matrix of system (9) satisfy the condition given in (36)

$$|\arg \sigma(J)| > \mu \frac{\pi}{2}. \quad (36)$$

In the Matignon criterion (36), the matrix  $J$  is the Jacobian matrix of the system (9),  $\sigma(J)$  is the set of all eigenvalues of  $J$ , and  $0 < \mu \leq 1$ , is the derivative order of (9).

Let us now fix the parameter values of the system as follows: Choose  $b = 1, c = 4, \alpha = a^2/bc = 50$ , and obtain the values of the remaining parameters based on the relation defined in (8). Consequently, the parameter values are selected as shown in (37):

$$\alpha = a^2/bc = 50, \quad \gamma = 1/b = 1, \quad \delta = -c^2/a^2 = -0.08, \quad \beta = -\delta\alpha. \quad (37)$$

The equilibrium points of (9) are given as follows:

- i. If  $\alpha < 1$ , the system (9) has a unique equilibrium point:  $E_0 = (0, 0, 0)$ ;
- ii. If  $\alpha > 1$ , the system (9) has three different equilibrium points given by  $E_0 = (0, 0, 0)$ ,

$$E_{1,2} = \left( \pm \frac{\beta\gamma\sqrt{\xi}}{\beta\gamma + \delta\xi}, \pm\sqrt{\xi}, \frac{\beta\xi}{\beta\gamma + \delta\xi} \right), \quad \xi = \frac{\beta\gamma}{2\delta^2} (\delta(\alpha - 2) - \beta + \sqrt{(\beta - \delta\alpha)^2 - 4\delta\beta}).$$

The Jacobian matrix of the system (9) is given by:

$$J = \begin{pmatrix} -\beta & \beta - \delta z & -\delta y \\ \alpha - z & -1 & -x \\ y & x & -\gamma \end{pmatrix} \quad \text{and} \quad J_0 = J(0, 0, 0) = \begin{pmatrix} -\beta & \beta & 0 \\ \alpha & -1 & 0 \\ 0 & 0 & -\gamma \end{pmatrix}.$$

The eigenvalues of  $J_0$  are given by:

$$\lambda_1 = -\gamma, \lambda_{2,3} = \frac{-(\beta + 1)}{2} \pm \frac{\sqrt{4\alpha\beta + (\beta - 1)^2}}{2}.$$

It is evident that the eigenvalues  $\lambda_1$  and  $\lambda_3$  are negative and thus satisfy the Matignon criterion (36). Moreover,  $\lambda_2 = -(\beta + 1)/2 + \sqrt{4\alpha\beta + (\beta - 1)^2}/2$ , meets the Matignon criterion for  $\alpha < 1$ . Thus, the equilibrium point  $E_0 = (0, 0, 0)$  is locally asymptotically stable for  $\alpha < 1$ .

Moreover, the eigenvalues of  $J_0$  for the parameter values shown in (37) are  $\lambda_1 = 11.7215, \lambda_2 = -16.7215, \lambda_3 = -1$ . Since  $\lambda_{2,3}$  satisfies the Matignon criterion for stability, we must check the case for  $\lambda_1 = 11.7215$ . The argument of  $\arg(\lambda_1) = 0$  and according to the Matignon criterion, 0 is outside the region of stability since  $0 < \mu\pi/2$ , for  $0 < \mu \leq 1$ . Therefore, the equilibrium point  $E_0 = (0, 0, 0)$  is locally unstable for the choice of the parameter values (37).

Likewise, the eigenvalues corresponding to the nontrivial equilibrium points  $E_{1,2}$  are  $\lambda_1 = 11.7213, \lambda_2 = -16.7214, \lambda_3 = -1$ . Therefore, it is evident that  $\lambda_{2,3}$  satisfies the Matignon criterion for stability and the argument of  $\arg(\lambda_1) = 0$  and according to the Matignon criterion, 0 is outside of the region of stability since  $0 < \mu\pi/2$ , for  $0 < \mu \leq 1$ . Therefore, the equilibrium points  $E_{1,2} = (\pm 0.0554, \pm 0.0554, 0.0031)$  are locally unstable for the choice of the parameter values (37).

**Table 1** Lyapunov exponents of the Rabinovich system for  $t \in [0, 300]$ , integration step of  $h = 0.01$ , normalization step of  $h$ -norm = 0.005

| Mu (fractional derivative order) | LE1     | LE2     | LE3      | Remark             |
|----------------------------------|---------|---------|----------|--------------------|
| 0.90                             | 0.4259  | 0.0058  | -10.4098 | Chaos              |
| 0.91                             | 0.0055  | -0.0903 | -9.3963  | Chaos              |
| 0.92                             | -0.0003 | -0.1707 | -8.8394  | Stable fixed point |
| 0.93                             | 0.0305  | -1.2642 | -7.3293  | Chaos              |
| 0.94                             | -0.0012 | -0.3615 | -7.7753  | Stable fixed point |
| 0.95                             | 0.0030  | -0.0224 | -7.7143  | Chaos              |
| 0.96                             | 0.0294  | -0.1121 | -7.2666  | Chaos              |
| 0.97                             | 0.0013  | -0.2441 | -6.7415  | Chaos              |
| 0.98                             | 0.0032  | -0.3599 | -6.2808  | Chaos              |
| 0.99                             | 0.0022  | -0.4941 | -5.8159  | Chaos              |
| 1.00                             | 0.0220  | -0.6391 | -5.3775  | Chaos              |

Summing up, the equilibrium points of the Rabinovich dynamic system (9) are locally unstable for the parameter values (37). In addition, the existence of one positive eigenvalue for each of the equilibrium points is a sufficient condition for a route to chaos.

## 6.2 Lyapunov exponents and Kaplan–Yorke dimension of the fractional-order Rabinovich system

This subsection describes Lyapunov exponents (LE) of the fractional Rabinovich dynamic system (10). The LEs are calculated using the Danca algorithm [25]. As mentioned above, the Matlab code developed by Danca obtains Lyapunov exponents of the fractional-order system in the Caputo fractional derivative using the predictor–corrector Adams–Bashforth–Moulton numerical scheme. The parameter values used are shown in (37), and the LEs for different values of the derivative order ( $\mu$ ) are shown in Table 1.

It is evident from Table 1 that the sum of the LEs in each row of the table is negative, and thus, the Rabinovich system (10) is dissipative. Moreover, for  $t \in [0, 300]$ , and the fractional derivative  $\mu \in (0.94, 1]$ , one of the LEs being positive indicates that the Rabinovich system exhibits chaotic behavior for the parameter values.

The Kaplan–Yorke dimension for some of the fractional derivatives considered in Table 1 is calculated as follows:

For the fractional-derivative order of 0.90,

$$\dim(LE) = 2 + \frac{0.4259 + 0.0058}{|-10.4098|} = 2.0415.$$

For the fractional-derivative order of 0.93,

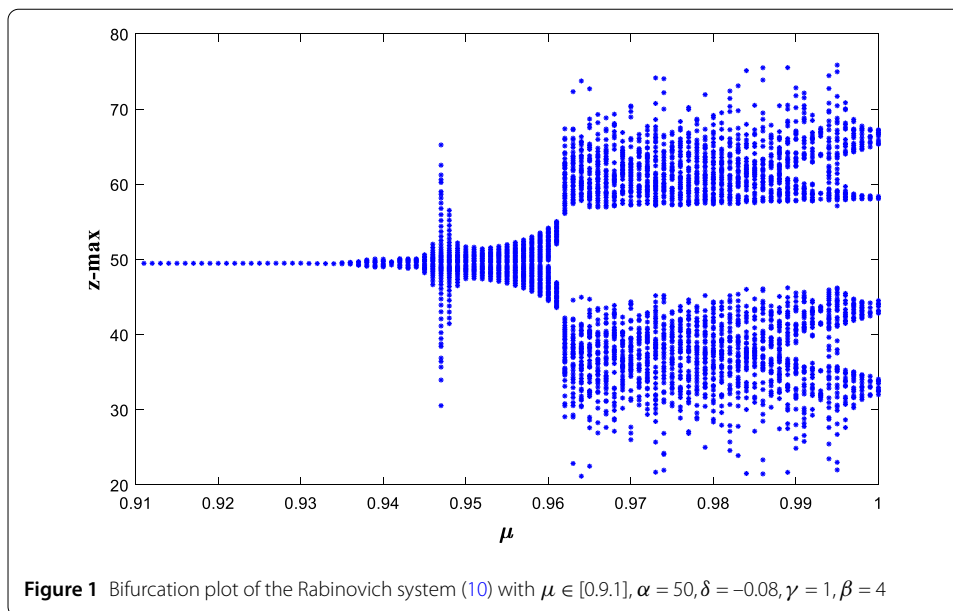
$$\dim(LE) = 1 + \frac{0.0305}{|-1.2642|} = 1.0241.$$

For the fractional-derivative order of 0.96,

$$\dim(LE) = 1 + \frac{0.0294}{|-0.1121|} = 1.2623.$$

For the fractional-derivative order of 0.99,

$$\dim(LE) = 1 + \frac{0.0022}{|-0.4941|} = 1.0045.$$



As can be seen, all the Kaplan–Yorke dimensions calculated above are fractions, and this result is an additional indication of the system’s route to chaos.

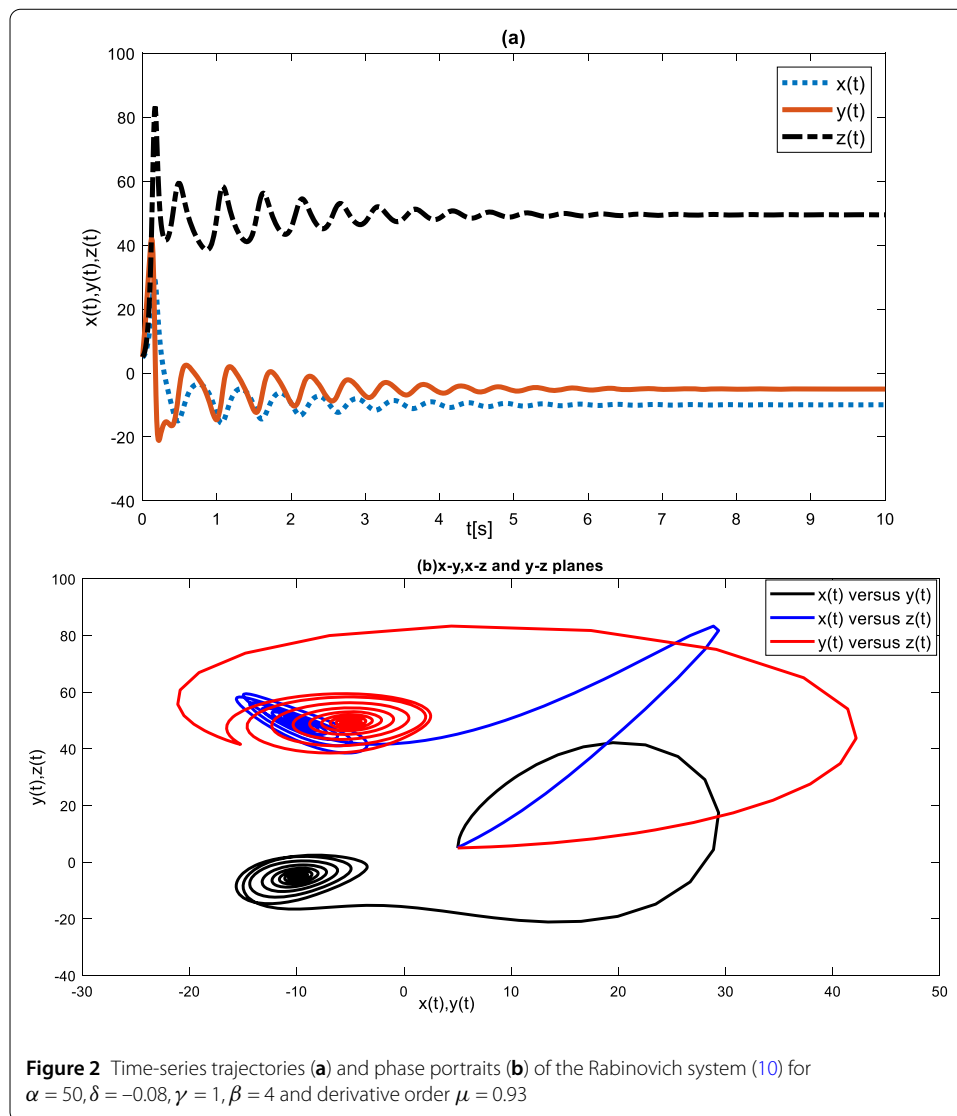
### 6.3 Bifurcation for fractional-derivative orders

This section describes the bifurcation diagram of the Rabinovich system with its fractional-derivative order supplemented by time-series trajectories and chaotic attractors with Caputo and ABC fractional derivatives. The bifurcation diagram for  $\mu \in [0.9, 1]$  and  $\alpha = 50$ ,  $\delta = -0.08$ ,  $\gamma = 1$ ,  $\beta = 4$  of the Rabinovich system is shown in Fig. 1. It is evident from Fig. 1 that the Rabinovich system undergoes chaos for the parameter values and the derivative orders of  $(0.940, 1]$ , with an integration step of  $h = 0.001$ . On the other hand, the system exhibits oscillation with stability for derivative-order values in the range  $[0.9, 0.940]$ .

Figures 2–11 verify the conclusion drawn from Fig. 1 for both the ABC and the Caputo context Rabinovich fractional-order system shown in (9) and (10). As seen from Fig. 2, time-series trajectory (a) and phase-space portrait (b), the system (10), in the sense of the Caputo fractional derivative, exhibits short time oscillation followed by stability for the fractional-derivative order 0.93 and the given parameter values.

It can be inferred from Fig. 3 that the ABC and the Caputo fractional-derivative representations of the system undergo oscillation with stability. However, it must be noted that the ABC representation’s oscillation time is shorter than the Caputo fractional-order representation of the Rabinovich system for the fractional-derivative order of  $\mu = 0.93$ ; this result agrees with the conclusion made from the bifurcation diagram.

It is evident from Fig. 4 that the Caputo Fractional-derivative representation of the system (10) exhibits an increasing number of periods, which is a clear route to chaos. Thus, the fractional representation of the Rabinovich system (10) is chaotic for a fractional-derivative order of 0.98 that agreed with the bifurcation diagram shown in Fig. 1. In addition, the chaotic nature of the system (10) is observed in the phase-space plot projected on different planes as shown in Fig. 5.

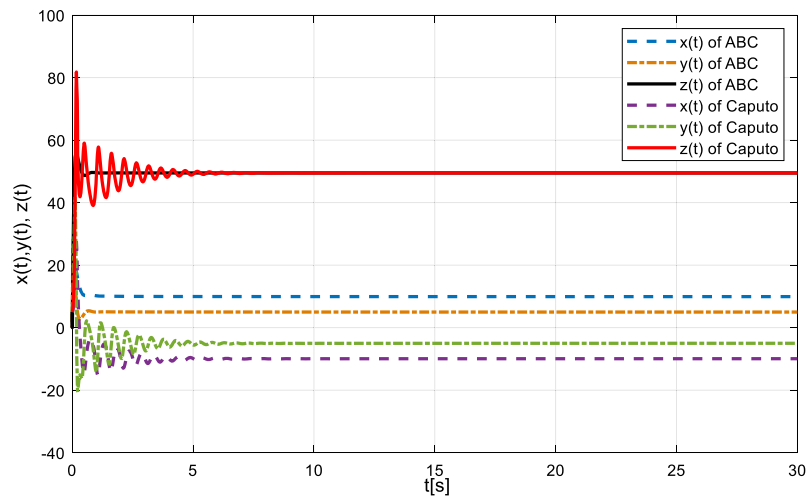


The time-series trajectories of the Rabinovich system in Caputo and ABC fractional-derivative representations for fractional-derivative order 0.994 shown in Fig. 6 display the system's chaotic nature in the context of both fractional derivatives. However, there is an observable difference in the significance of chaos between the two representations (9) and (10) of the Rabinovich system; the quantity of the chaos is remarkably different in each case. This difference is depicted in the attractors shown in Fig. 7 (via ABC) and Fig. 8 (via Caputo) for a derivative order of 0.994.

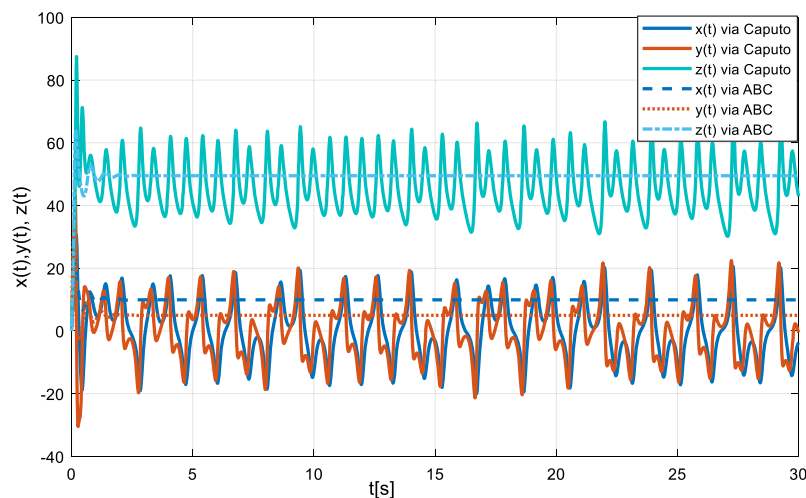
From Figs. 9 and 10, we see that both the fractional-order representations undergo chaotic behavior. However, it seems that the Caputo context chaotic nature (Figs. 9(a), (b), (c), and (g)) is more significant than the ABC case chaotic nature (Figs. 9(d), (e), (f), and h) for a fractional-derivative order of 0.998.

Figure 11 depicts the time-series trajectories ((a) and (b)) and attractors (b and (c)) of the fractional Rabinovich system for a fractional order of 1. In this case, it seems that the ABC and Caputo context representations of the Rabinovich system exhibit significant chaotic nature.





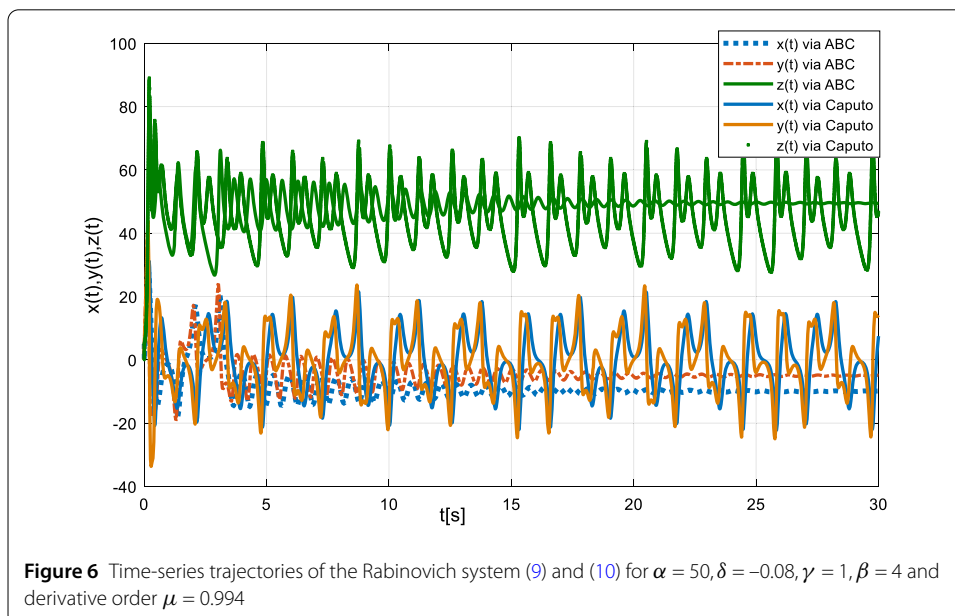
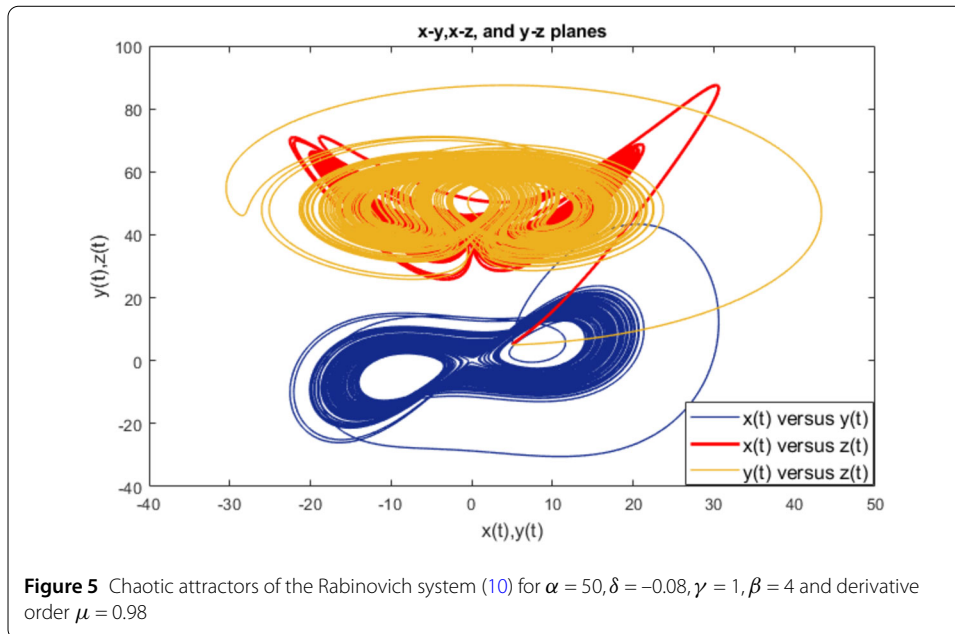
**Figure 3** Time-series trajectories of the Rabinovich system (9) and (10) for  $\alpha = 50, \delta = -0.08, \gamma = 1, \beta = 4$  and derivative order  $\mu = 0.96$



**Figure 4** Rabinovich system's (9) and (10) time-series trajectories for  $\alpha = 50, \delta = -0.08, \gamma = 1, \beta = 4$  and derivative order  $\mu = 0.98$

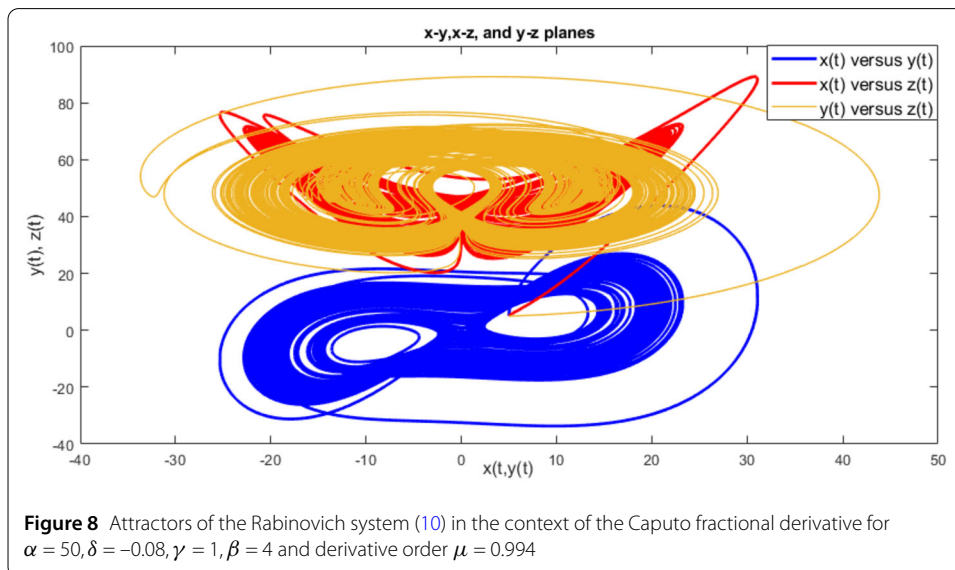
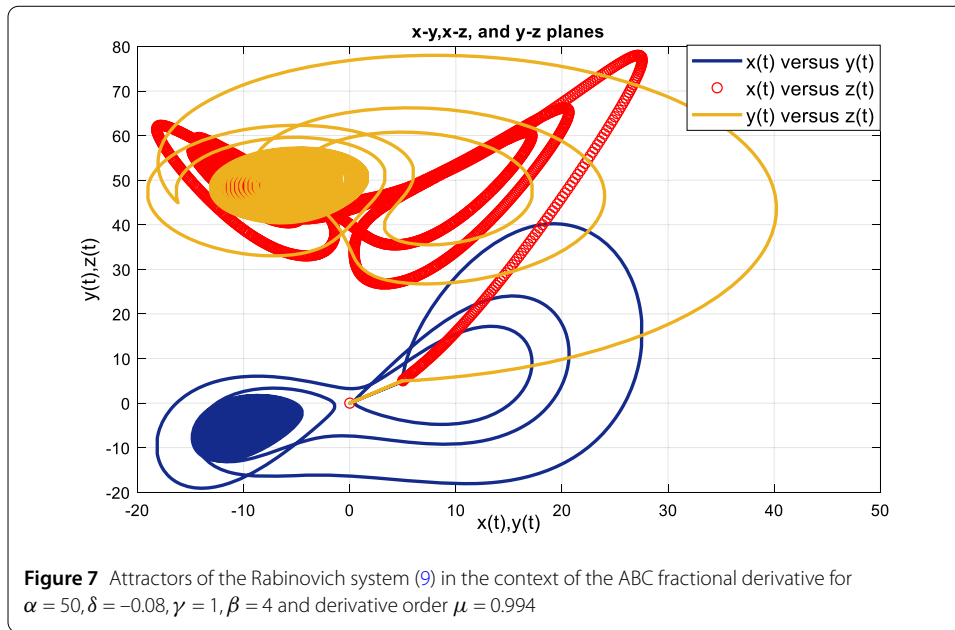
#### 6.4 On the sensitivity to initial conditions of the fractional-order Rabinovich system

In this section of the study, the impact of different initial conditions on the dynamics of the chaotic Rabinovich system through the Caputo and ABC fractional derivatives is examined. Chaotic attractors are described by sensitivity to small changes of the system's initial and parameter values, strong harmonics among the trajectories, fractional Kaplan–Yorke dimension, and at least one positive Lyapunov exponent showing a stretching direction of the system. Thus, it is appropriate to examine the sensitivity to initial values of systems (9) and (10). To explore the sensitivity to initial conditions of the systems (9) and (10), three different initial conditions were used:  $X_0 = (5; 5; 5), (5.01; 5.01, 5.01)$ , and  $(4.55; 4.55; 4.55)$  for simulation graphs. The corresponding time-series trajectories are depicted in Fig. 12



(via the Caputo fractional derivative) and Fig. 13 (via the ABC fractional derivative). It is evident from the figures that the systems are strongly dependent on initial conditions. However, the degree of sensitivity is different between the two fractional derivatives.

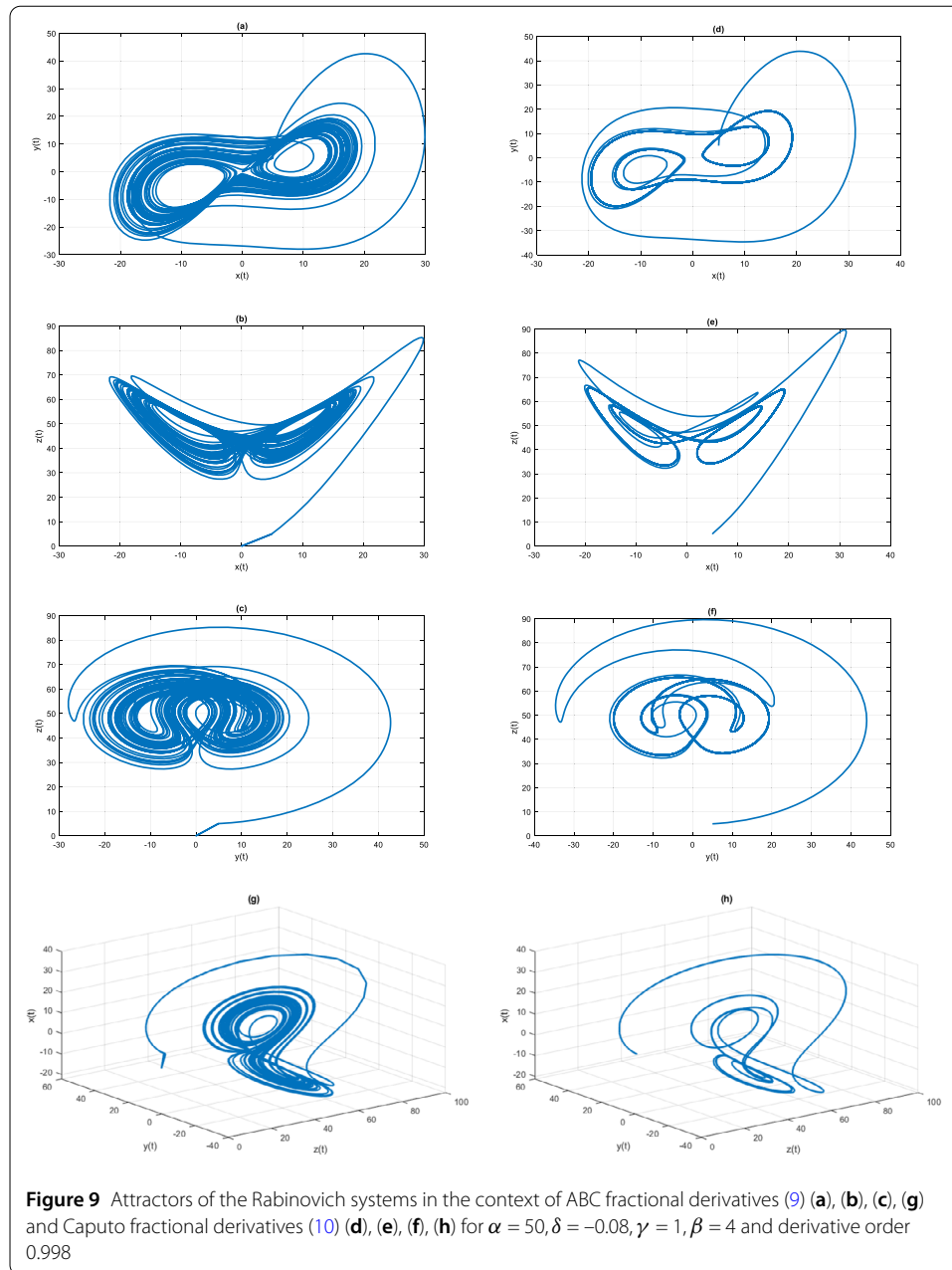
The ABC context Rabinovich system time-series trajectories started divergence before the Caputo context Rabinovich system trajectories, as seen in Figs. 12 and 13. From Fig. 12, the  $x(t)$  and  $y(t)$  seem to overlap over the first 20-second simulation, and that is not the case for Fig. 13 a; they seem to overlap only for the first 8 seconds. The same difference exists between Figs. 12b and 13b.



## 7 Synchronization of the Rabinovich system via ABC fractional derivatives

In this part of the study, a master–response system of the Rabinovich system given in (9) through the ABC fractional derivative is designed. First, a coupling function is developed to associate two identical copies of the Rabinovich system (9). Secondly, the two systems are simulated using two different initial conditions. The simulation resulted in time-series trajectories and phase-space plots of the master and the response systems, showing a strong correlation. Moreover, the error dynamics resulted in a linear system whose coefficient matrix has negative eigenvalues, demonstrating the error's asymptotic stability.

The following concept is used for developing the master–response relationship between identical copies of the Rabinovich system (9).



Let the master and the response systems be given by Eqs. (38) and (39)

$$\dot{X} = f(X), \quad (38)$$

$$\dot{X}_s = F(X_s) + C + \left( \frac{\partial F}{\partial X} - H \right) (X - X_s), \quad (39)$$

where  $H$  is an arbitrary Hermitian matrix of appropriate size,  $\partial F / \partial X$  is the Jacobian matrix of the master system,  $C + (\partial F / \partial X - H)(X - X_s)$  is the coupling function, and  $C = (c_1, c_2, c_3)$ ,  $X = (x, y, z)$ ,  $X_s = (x_s, y_s, z_s)$ .

The error is defined as  $\zeta = (e_1, e_2, e_3) = X - X_s = (x - x_s, y - y_s, z - z_s)$ . Now, to verify if the error dynamics of the synchronization process is asymptotically stable, we proceed as

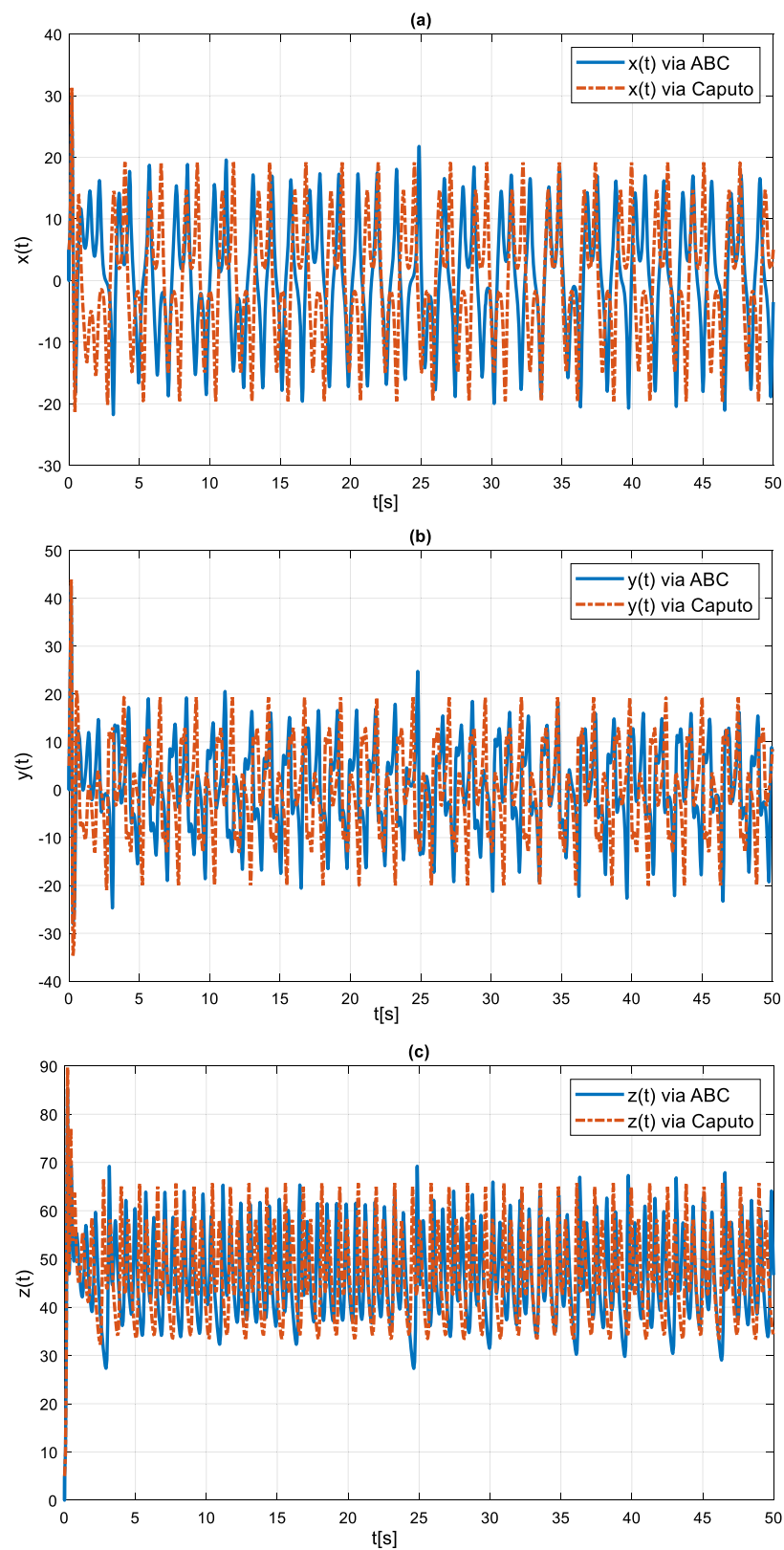


**Figure 10** Time-series trajectories of the Rabinovich system via Caputo (10) and ABC fractional derivatives (9) for  $\alpha = 50, \delta = -0.08, \gamma = 1, \beta = 4$  and derivative order 0.998

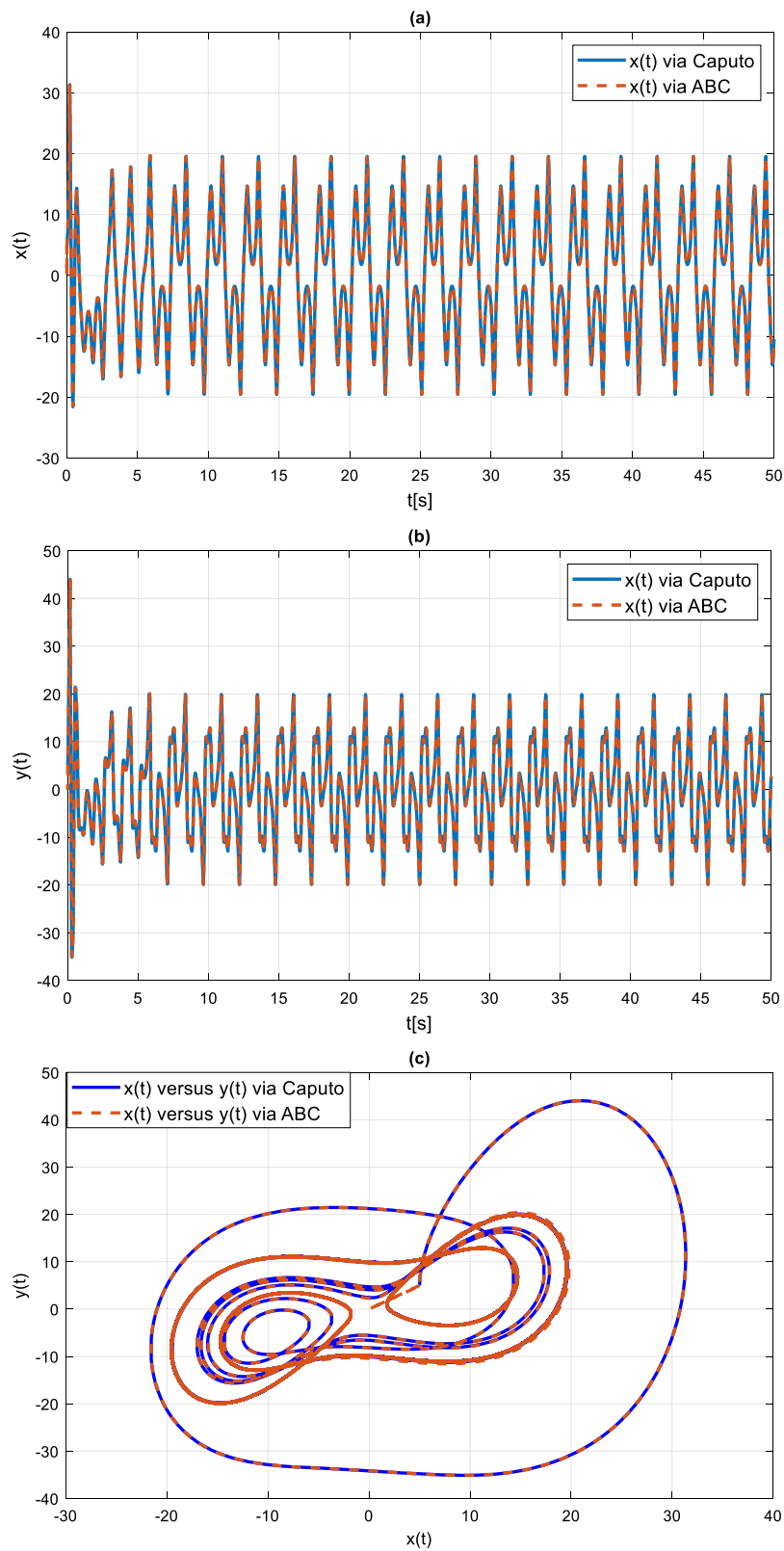
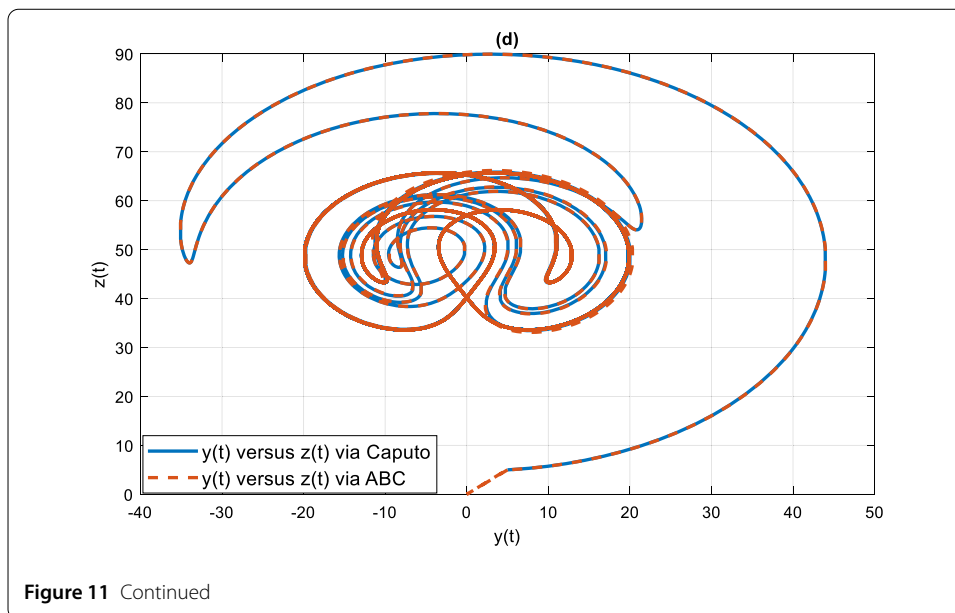


**Figure 11** Time-series trajectories of the Rabinovich system via Caputo (10) and ABC fractional derivatives (9) for  $\alpha = 50, \delta = -0.08, \gamma = 1, \beta = 4$  and derivative order 1



follows.

$$\begin{aligned}\dot{\zeta} &= \dot{X} - \dot{X}_s = F(X) - F(X_s) - \left( \frac{\partial F}{\partial X} - H \right) (X - X_s) - C \\ &= F(X) - \left( F(X_s) + \frac{\partial F}{\partial X} (X - X_s) \right) - \frac{\partial F}{\partial X} (X - X_s) + H(X - X_s) - C.\end{aligned}$$

By making an appropriate choice for the matrix  $C$ , we can reduce the error dynamics to the equality (40)

$$\dot{\zeta} = H\zeta \Rightarrow \zeta(t) = e^{Ht}. \quad (40)$$

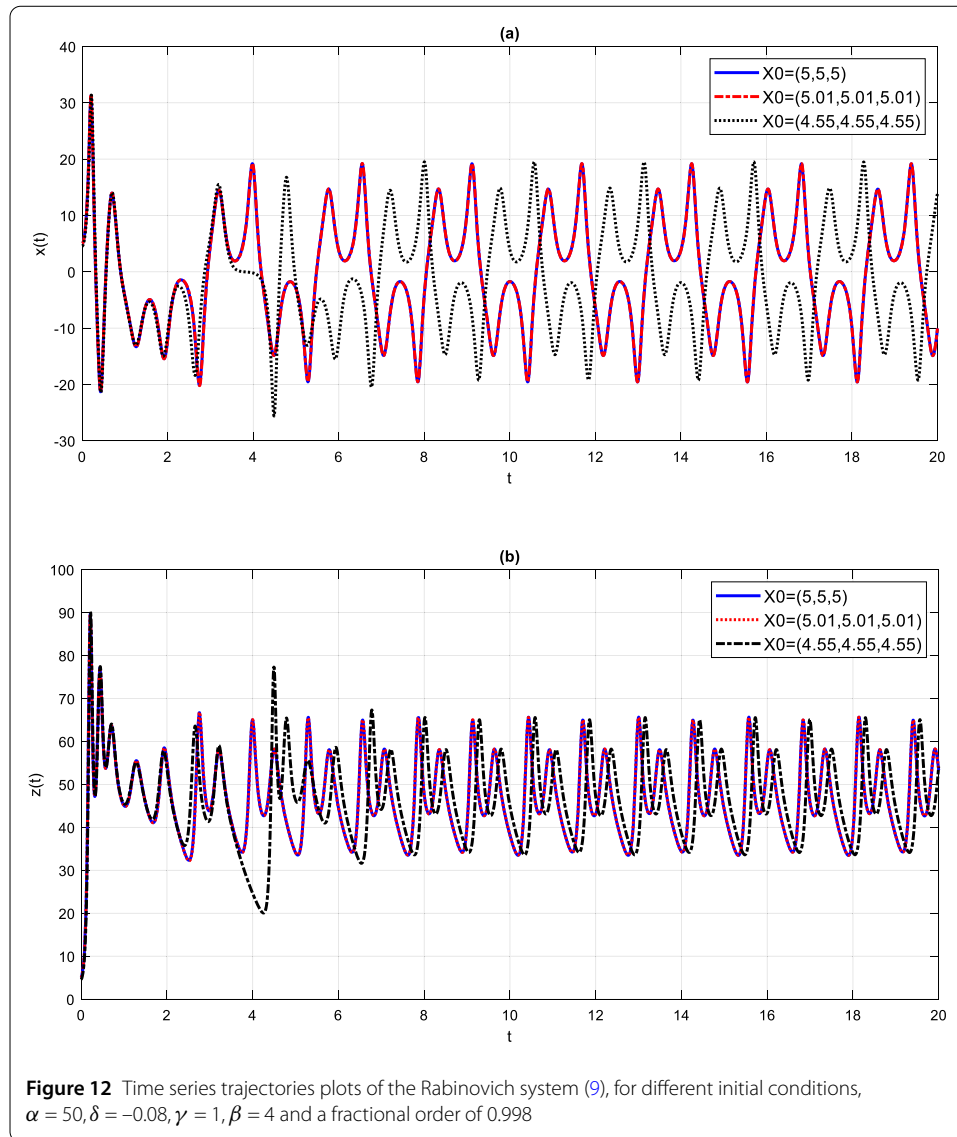
Since the eigenvalues of the Hermitian matrix  $H$  have a negative real part, the error dynamics of the synchronization is globally asymptotically stable.

Based on the above-explained synchronization process, let the master Rabinovich system be as in (41)

$$\begin{aligned}{}_0^{ABC}D_t^\mu x(t) &= \beta(y - x) - \delta yz, \\ {}_0^{ABC}D_t^\mu y(t) &= \alpha x - y - xz, \\ {}_0^{ABC}D_t^\mu z(t) &= -\gamma z + xy.\end{aligned} \quad (41)$$

Define the response system as in (42)

$$\begin{cases} {}_0^{ABC}D_t^\mu x_s(t) = \beta(y_s - x_s) - \delta y_s z_s + c_1, \\ {}_0^{ABC}D_t^\mu y_s(t) = \alpha x_s - y_s - x_s z_s + c_2, \\ {}_0^{ABC}D_t^\mu z_s(t) = -\gamma z_s + x_s y_s + c_3, \end{cases} + \left( \frac{\partial F}{\partial X} - H \right) (X - X_s), \quad (42)$$



where the coupling function is given by

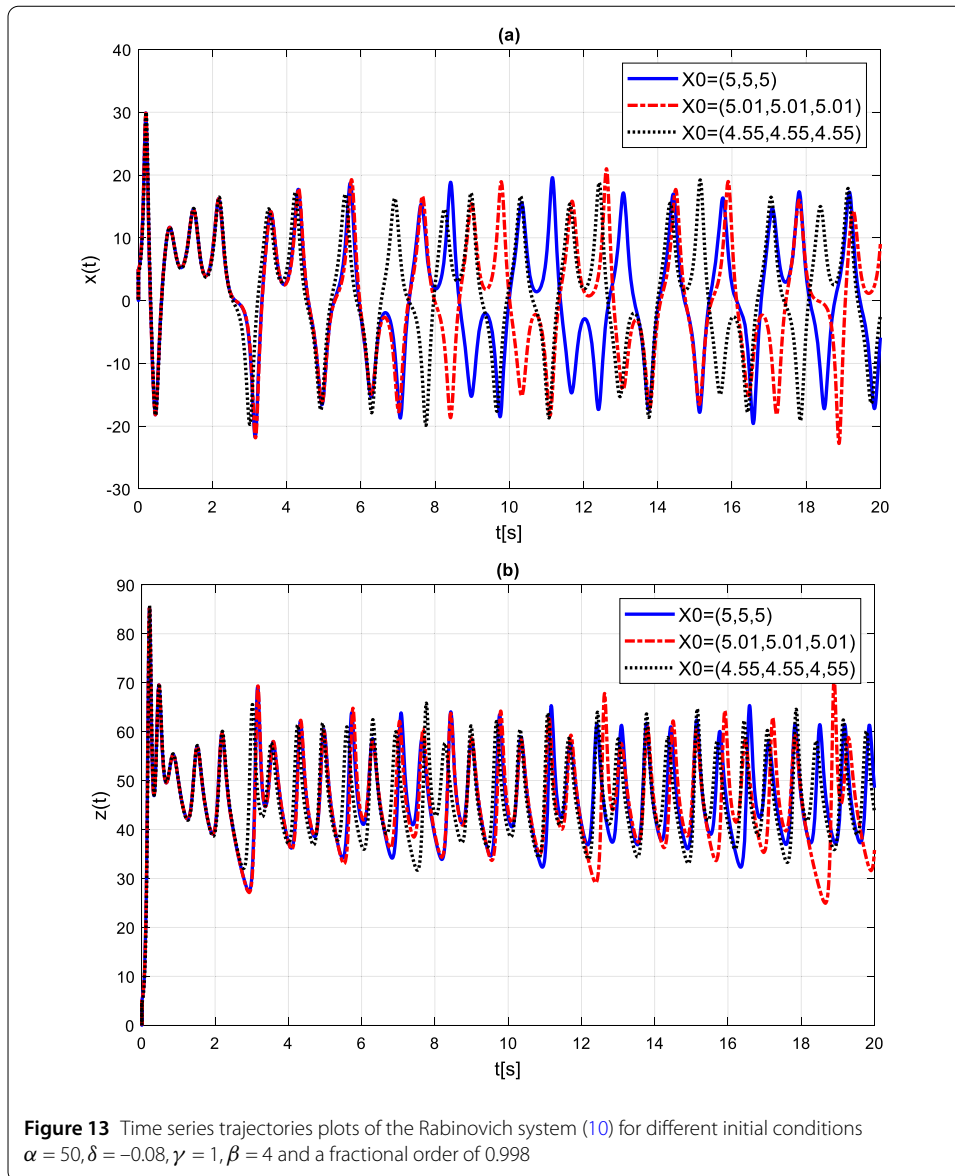
$$\left( \frac{\partial F}{\partial X} - H \right) (X - X_s) = \begin{pmatrix} c_1 \\ c_2 \\ c_3 \end{pmatrix} + \begin{pmatrix} -1 - \beta & -2 + \beta - \delta z & -\delta y \\ 27 + \alpha - z & 26 & -x \\ y & x & 2 - \gamma \end{pmatrix} \begin{bmatrix} x - x_s \\ y - y_s \\ z - z_s \end{bmatrix}.$$

The Hermitian matrix  $H$  is chosen to be

$$H = \begin{bmatrix} 1 & 2 & 0 \\ -27 & -27 & 0 \\ 0 & 0 & -2 \end{bmatrix}.$$

The eigenvalues of the Hermitian matrix  $H$  are given by  $\lambda_1 = -1.0836, \lambda_2 = -24.9164, \lambda_3 = -2$ . Since all the eigenvalues of the matrix  $H$  are negative, and the Matignon criterion is met,  $H$  is a Hermitian matrix.





Adding the coupling function to the system (42), the response system now evolves to Eq. (43)

$$\begin{cases} {}^{ABC}_0 D_t^\mu x_s(t) = (x_s - x) + \beta(y - x) - (\delta z + 2)(y - y_s) - \delta y(z - z_s) - \delta y_s z_s + c_1, \\ {}^{ABC}_0 D_t^\mu y_s(t) = 27(x - x_s) + x(z_s - 2z) + x_s(z - z_s) + \alpha x + 26y - 27y_s + c_2, \\ {}^{ABC}_0 D_t^\mu z_s(t) = -y(x_s - x) - x(y_s - y) - 2(z_s - z) - \gamma z + x_s y_s + c_3. \end{cases} \quad (43)$$

Based on Eqs. (41), (43), and the definition of the error dynamics (40), we have the error dynamics given by (44)

$$\begin{cases} {}^{ABC}_0 D_t^\mu e_1 = e_1 + 2e_2 + \delta e_2 e_3 - c_1, \\ {}^{ABC}_0 D_t^\mu e_2 = -27e_1 - 27e_2 + e_1 e_3 - c_2, \\ {}^{ABC}_0 D_t^\mu e_3 = -2e_3 - e_1 e_2 - c_3. \end{cases} \quad (44)$$

Let us choose  $c_i, i = 1, 2, 3$  from (44) as follows:

$$\begin{pmatrix} c_1 \\ c_2 \\ c_3 \end{pmatrix} = \begin{pmatrix} \delta e_2 e_3 \\ e_3 e_1 \\ -e_1 e_2 \end{pmatrix}. \quad (45)$$

The error dynamics reduces to the system (46)

$$\begin{pmatrix} {}^{ABC}_0 D_t^\mu e_1 \\ {}^{ABC}_0 D_t^\mu e_2 \\ {}^{ABC}_0 D_t^\mu e_3 \end{pmatrix} = \begin{pmatrix} 1 & 2 & 0 \\ -27 & -27 & 0 \\ 0 & 0 & -2 \end{pmatrix} \begin{pmatrix} e_1 \\ e_2 \\ e_3 \end{pmatrix}. \quad (46)$$

Finally, the response system (42) becomes

$$\begin{cases} {}^{ABC}_0 D_t^\mu x_s(t) = \beta(y - x) - \delta zy + (x_s - x) - 2(y - y_s), \\ {}^{ABC}_0 D_t^\mu y_s(t) = 27(x - x_s) - xz + \alpha x + 26y - 27y_s, \\ {}^{ABC}_0 D_t^\mu z_s(t) = xy + 2(z - z_s) - \gamma z. \end{cases} \quad (47)$$

The following section depicts the phase portraits of the master system (41) and response systems (47). The parameter values used for the simulation are  $\alpha = 50, \gamma = 1, \delta = -0.08, \beta = 4$ , and the fractional derivative is  $\mu = 0.998$ . The initial condition for the master system, and the response systems are, respectively,  $X_0 = (5, 5, 5)$  and  $X_{s0} = (-10, -10, -10)$ . The Toufik–Atangana numerical scheme is used for approximating the solutions of the systems.

As can be seen from time-series trajectories in Figs. 14(a)–(c) and the phase-space plots in Figs. 15(a) and (b) and their respective zooming in, shown in Figures 15(a1) and (b1), the master system (41) and the response system (47) have an excellent correlation. As shown in Fig. 14, the trajectories come close to each other after about 3 seconds of the simulation time. The zooming in of Figures 15(a1) and (b1) vividly shows the strong relationship between the two systems.

## 8 Conclusion

In this report, a qualitative analysis of the 3D fractional-order Rabinovich dynamical system is accomplished in the context of ABC and Caputo fractional-order derivatives. The Lyapunov exponents for fractional derivative (9) discovered that the fractional Rabinovich system exhibits a chaotic behavior for fractional-derivative orders in the interval  $[0.9, 1]$ . In the ABC context, the Rabinovich system shows a chaotic behavior for fractional-order derivatives in the interval  $[0.994, 1]$  for the parameter values given in (37); see Figs. 2–10. The overall conclusion is that the ABC case becomes chaotic slower than the Caputo case of the system. As the fractional derivative gets close to 1, the significance of the chaos for the ABC case increases and becomes as significant as that of the Caputo representation of the system. At the fractional-derivative order of 1, the Rabinovich system's fractional models (9) and (10) show approximately the same behavior; see Fig. 11. It must be clear that the Lyapunov exponents, the bifurcation diagrams, time-series trajectories, and phase-space plots related to the Caputo fractional-derivative representation of the Rabinovich system were carried out using the Danca algorithm [25] and numerical method of Garrappa [24].

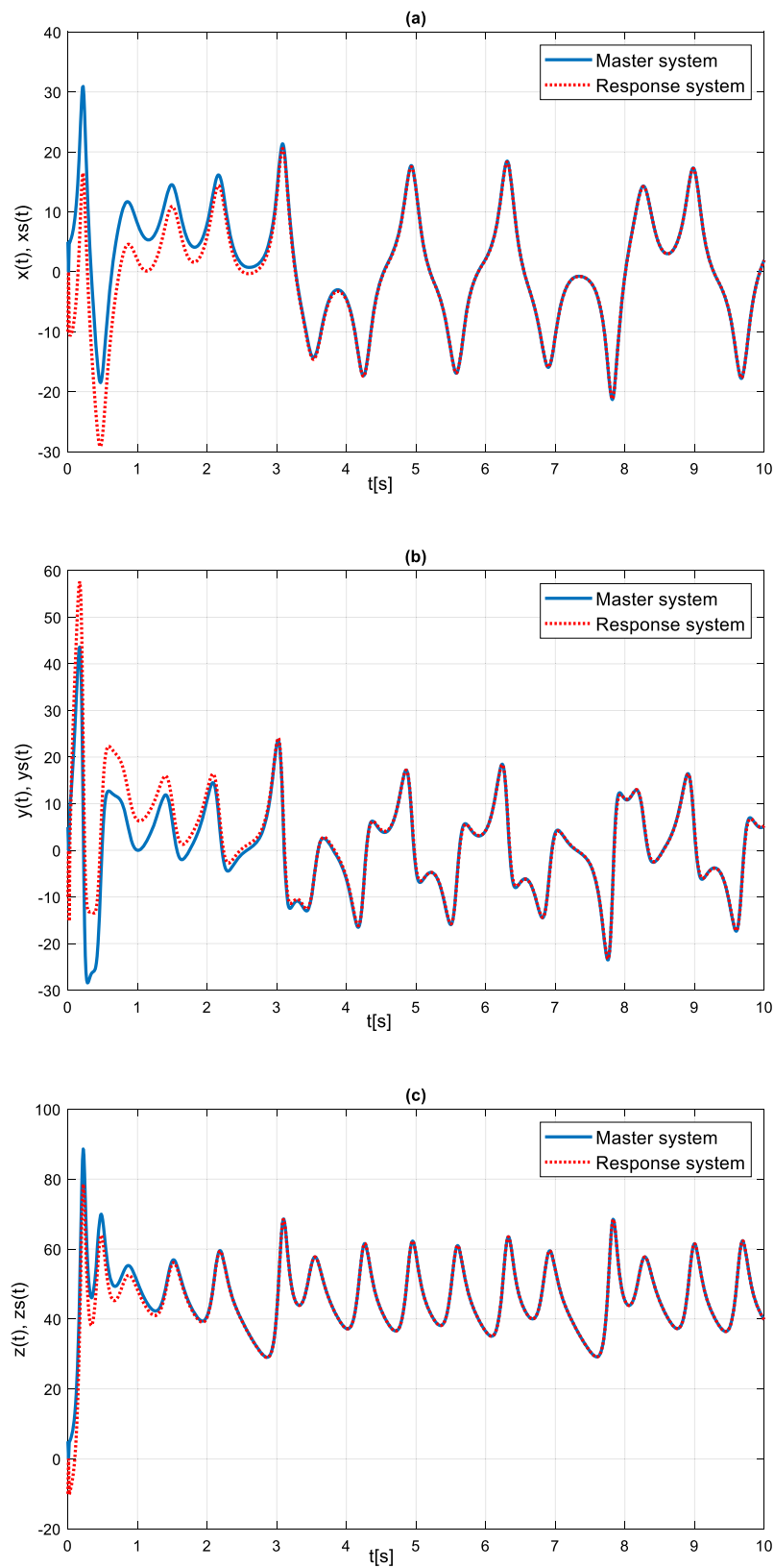


**Figure 14** Time-series trajectories of the master and the response systems of (41) and (47)

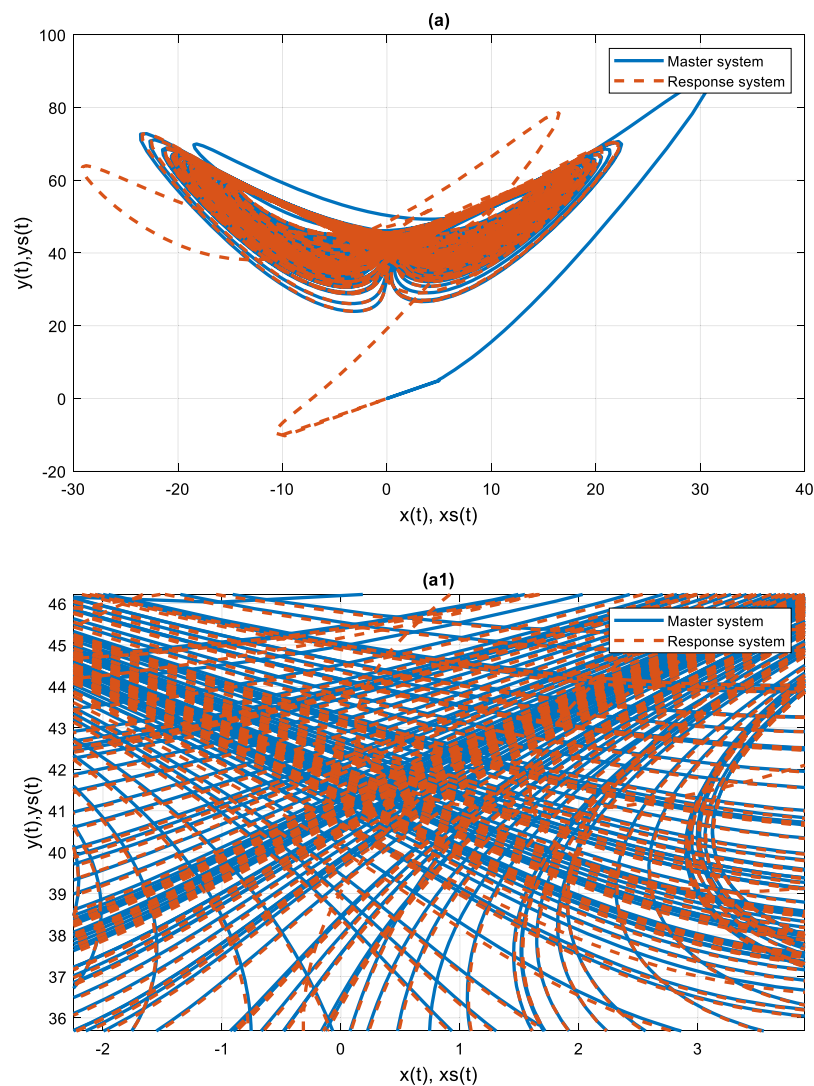


**Figure 15** Phase-space plots of the master (41) and the response (47) systems with their corresponding zooming in (a1) and (b1) of (a) and (b), respectively

In this case, the Adams–Bashforth–Moulton numerical scheme is applied to develop the Matlab code. On the other hand, all simulation results in this report related to the ABC fractional-derivative representation of the Rabinovich system are carried out using the Toufik–Atangana numerical scheme for fractional derivatives [23].

The master–response synchronization process developed in this report showed the applicability of the fractional Rabinovich system for secure communications and other related practical applications. Furthermore, the author believes that this study exposed hidden behaviors of the Rabinovich system using the two fractional-derivative concepts, which is not possible in the integer-derivative case. Moreover, although this research’s objective was not to compare the two fractional-derivative concepts and the corresponding numerical schemes applied, a significant difference is observed in using the ABC and Caputo fractional derivatives for the Rabinovich system, as explained above. Therefore,

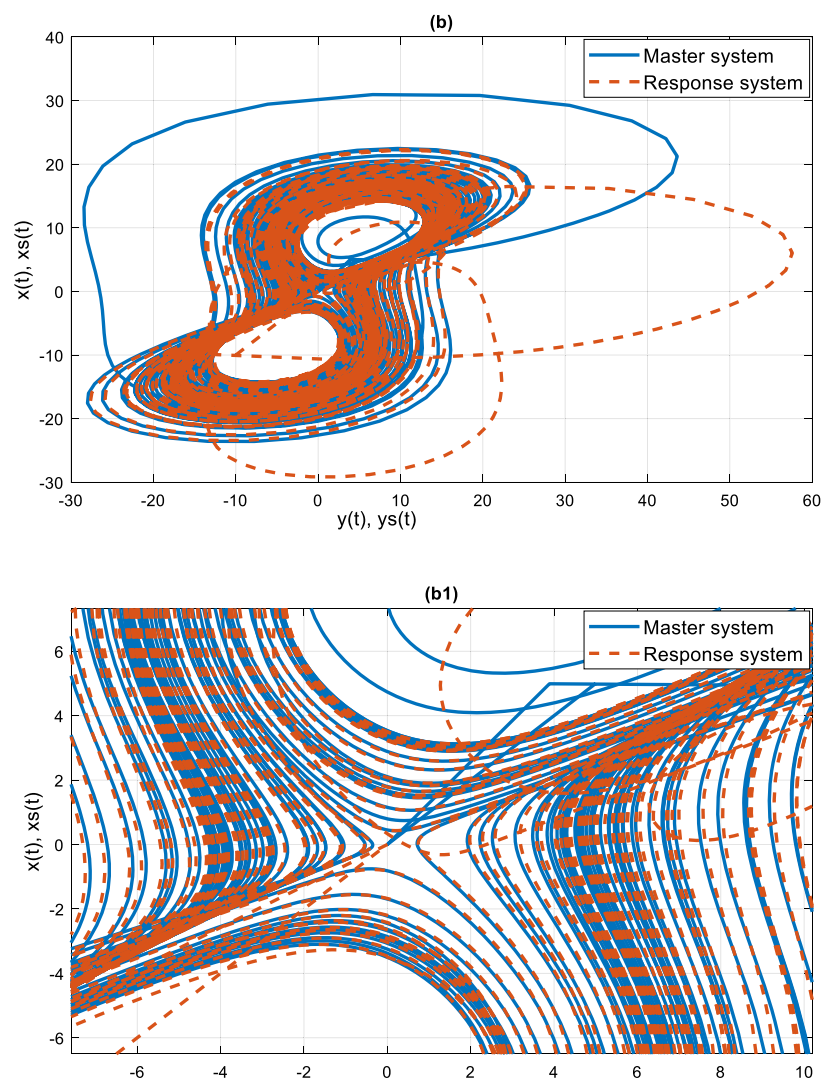


Figure 15 Continued

future work could compare the effects of applying different fractional-derivative concepts to the same dynamic system.

#### Acknowledgements

The author would like to thank the College of Natural Sciences, Jimma University, Ethiopia.

#### Funding

This study was not funded by any organization.

#### Availability of data and materials

No dataset was generated or analyzed in the current study.

#### Declarations

##### Competing interests

The author declares that there is no conflict of interest.

##### Author contribution

The author has done all the activities in this study, read, and approved the final manuscript.

## Publisher's Note

Springer Nature remains neutral with regard to jurisdictional claims in published maps and institutional affiliations.

Received: 14 January 2022 Accepted: 16 November 2022 Published online: 30 November 2022

## References

1. Deressa, C.T., Duressa, G.F.: Analysis of Atangana–Baleanu fractional-order SEAIR epidemic model with optimal control. *Adv. Differ. Equ.* **2021**, Article ID 174 (2021)
2. Rezapour, S., Deressa, C.T., Etemad, S.: On a memristor-based hyperchaotic circuit in the context of nonlocal and nonsingular kernel fractional operator. *J. Math.* **2021**, Article ID 6027246 (2021)
3. Deressa, C.T., Etemad, S., Rezapour, S.: On a new four-dimensional model of memristor-based chaotic circuit in the context of nonsingular Atangana–Baleanu–Caputo operators. *Adv. Differ. Equ.* **2021**, Article ID 444 (2021)
4. Guo, R., Zhang, Y., Jiang, C.: Synchronization of fractional-order chaotic systems with model uncertainty and external disturbance. *Mathematics* **9**(8), Article ID 877 (2021)
5. Effah-Poku, S., Obeng-Denteh, W., Dontwi, I.K.: A study of chaos in dynamical systems. *J. Math.* **2018**, Article ID 1808953 (2018)
6. Banks, J., Brooks, J., Cairns, G., Davis, G., Stacey, P.: On Devaney's definition of chaos. *Am. Math. Mon.* **99**(4), 332–334 (1992)
7. Azar, A.T., Vaidyanathan, S. (eds.): *Advances in Chaos Theory and Intelligent Control*. Springer, Berlin (2016)
8. Belozyorov, V.: Research of chaotic dynamics of 3D autonomous quadratic systems by their reduction to special 2D quadratic systems. *Math. Probl. Eng.* **2015**, Article ID 271637 (2015)
9. Shaukat, S., Arshid, A.L., Eleyan, A., Shah, S.A., Ahmad, J.: Chaos theory and its application: an essential framework for image encryption. *Chaos Theory Appl.* **30**(2), 17–22 (2020)
10. Ayers, S.: The application of chaos theory to psychology. *Theory Psychol.* **7**(3), 373–398 (1997)
11. Alam, Z., Yuan, L., Yang, Q.: Chaos and combination synchronization of a new fractional-order system with two stable node-foci. *IEEE/CAA J. Autom. Sin.* **12**(3), 157–164 (2016)
12. Sun, K., Wang, X., Sprott, J.C.: Bifurcations and chaos in fractional-order simplified Lorenz system. *Int. J. Bifurc. Chaos* **20**(04), 1209–1219 (2010)
13. Kumar, S., Singh, C., Prasad, S.N., Shekhar, C., Aggarwal, R.: Synchronization of fractional order Rabinovich–Fabrikant systems using sliding mode control techniques. *Arch. Control Sci.* **29**, 307–322 (2019)
14. Kuznetsov, N.V., Leonov, G.A., Mokaev, T.N., Prasad, A., Shrimali, M.D.: Finite-time Lyapunov dimension and hidden attractor of the Rabinovich system. *Nonlinear Dyn.* **92**(2), 267–285 (2018)
15. Akgül, A., Modanli, M.: On solutions of fractional telegraph model with Mittag–Leffler kernel. *J. Comput. Nonlinear Dyn.* **17**(2), Article ID 021006 (2022)
16. Akgül, A., Modanli, M.: Crank–Nicholson difference method and reproducing kernel function for third-order fractional differential equations in the sense of Atangana–Baleanu Caputo derivative. *Chaos Solitons Fractals* **127**, 10–16 (2019)
17. Modanli, M.: Comparison of Caputo and Atangana–Baleanu fractional derivatives for the pseudo hyperbolic telegraph differential equations. *Pramana* **96**(1), 1–8 (2022)
18. Matignon, D.: Stability results for fractional differential equations with applications to control processing. In: *Computational Engineering in Systems Applications*, vol. 2, pp. 963–968 (1996)
19. Atangana, A., Baleanu, D.: New fractional derivatives with nonlocal and nonsingular kernel: theory and application to heat transfer model. *arXiv preprint*. [arXiv:1602.03408](https://arxiv.org/abs/1602.03408)
20. Diethelm, K., Ford, N.J.: Analysis of fractional differential equations. *J. Math. Anal. Appl.* **15**(265), 229–248 (2002)
21. Kilbas, A.A., Srivastava, H.M., Trujillo, J.J.: *Theory and Applications of Fractional Differential Equations*. Elsevier, Amsterdam (2006)
22. Granas, A., Dugundji, J.: Elementary fixed point theorems. In: *Fixed Point Theory*, pp. 9–84. Springer, New York (2003)
23. Toufik, M., Atangana, A.: New numerical approximation of fractional derivative with non-local and nonsingular kernel: application to chaotic models. *Eur. Phys. J. Plus* **132**(10), 1–6 (2017)
24. Garrappa, R.: Numerical solution of fractional differential equations: a survey and a software tutorial. *Mathematics* **6**(2), Article ID 16 (2018)
25. Danca, M.F., Kuznetsov, N.: Matlab code for Lyapunov exponents of fractional-order systems. *Int. J. Bifurc. Chaos* **28**(05), Article ID 1850067 (2018)

**Submit your manuscript to a SpringerOpen<sup>®</sup> journal and benefit from:**

- Convenient online submission
- Rigorous peer review
- Open access: articles freely available online
- High visibility within the field
- Retaining the copyright to your article

---

Submit your next manuscript at ► [springeropen.com](https://www.springeropen.com)